



Heat and Mass Transfers on the Chemically Reactive Thermosolutal Convective Flow of Rivlin-Ericksen Fluid over a Porous Medium with Viscous Dissipation Effect

A. M Mohamad^a, Dhananjay Yadav^{a,*}, Mukesh Kumar Awasthi^b, Ravi Ragoju^c,
Mohammad Hassan^d

^a Department of Mathematical & Physical Sciences, University of Nizwa, Oman

^b Department of Mathematics, Babasaheb Bhimrao Ambedkar University, Lucknow 226025, India

^c Department of Applied Sciences, National Institute of Technology Goa, Goa, 403401, India

^d Department of Mathematics and Scientific Computing, Madan Mohan Malaviya University of Technology, Gorakhpur-273010, UP, India

Abstract

Chemically reacting flows of non-Newtonian fluids through porous media have numerous medical and industrial applications, including targeted drug delivery, polymer processing, and extrusion operations. In these contexts, convective heat transfer is a critical mechanism that must be accurately predicted. This article analyzes the thermosolutal convection of a chemically reactive Rivlin-Ericksen fluid in a porous medium, accounting for viscous dissipation, using both linear and nonlinear stability approaches. The nonlinear analysis is performed using a truncated Fourier series method, while the linear stability is examined via the normal mode technique. It is found that oscillatory convection occurs only when the solutal Rayleigh-Darcy number is negative. The range of this number that allows oscillatory convection depends on several physical parameters. An increase in the Rivlin-Ericksen parameter, the modified heat capacity ratio, and the Péclet number reduces this range, whereas a higher Lewis number expands it. Moreover, the Lewis number, solutal Rayleigh-Darcy number, and Gebhart number accelerate the onset of convective waves, while the Rivlin-Ericksen parameter and the modified heat capacity ratio delay it. Additionally, both convective heat and mass transfer rates decrease with increasing Rivlin-Ericksen parameter and modified heat capacity ratio, but they increase with higher values of the thermal and solutal Rayleigh-Darcy numbers, the Lewis number, the chemical reaction parameter, the Péclet number, and the Gebhart number.

Keywords: Rivlin-Ericksen fluid; Thermosolutal convection; viscous dissipation; Porous media; Chemical reaction; Nonlinear stability analysis;

* Corresponding author, E-mail address: dhananjayadav@gmail.com

1. Introduction

Thermal instability, or convective instability, in Rivlin-Ericksen fluids is crucial for understanding heat and mass transmission in non-Newtonian fluids, often encountered in polymeric solutions and industrial processes. This study aids in analysing the arrival of convection driven by temperature and solute gradients, considering the viscoelastic properties unique to Rivlin-Ericksen fluids, and is vital for applications in material processing, geophysical flows, and enhanced energy systems. The Rivlin-Ericksen (R-E) fluid, a kind of viscoelastic liquid, was initially introduced theoretically by Rivlin and Ericksen [1] in 1955. Sharma and Kumar [2] investigated the thermal convection of a Rivlin-Ericksen fluid under the influence of uniform rotation. In another investigation, Sharma and Kumar [3] explored the thermal convection of Rivlin-Ericksen liquid in the attendance of a constant magnetic field. Sharma et al. [4-6] utilized normal mode philosophy to investigate the thermal convection of a Rivlin-Ericksen liquid layer under various conditions, including porous media, and Hall effects. Gupta and Sharma [7] further extended the analysis by incorporating extra features such as concentration, compressibility, Hall influence, and rotation into the study of thermal instability. Kango and Singh [8] contributed by including the outcomes of a magnetic power and permeable medium in their investigation.

Thermosolutal instability in Rivlin-Ericksen fluid plays a crucial role in analysing heat and mass spread processes in viscoelastic fluids, with significant applications in polymer processing, chemical engineering, and geophysical fluid dynamics. This instability provides insights into the collective effects of heat and solutal gradients on the stability of fluid layers, helping optimize industrial processes involving complex fluids. Sharma and Chand [9] examined thermosolutal convective drive in a porous medium occupied with Rivlin-Ericksen fluid, predisposed by a constant upright magnetic field. They instituted that the solutal gradient and magnetic power stabilized the system, while the medium's permeability had a non-stabilizing influence. Kinematic viscoelasticity did not affect stationary convection, but oscillatory modes appeared when a stable solutal gradient and magnetic power were ensued. Kishor and Sharma [10] studied the collective effects of Hall currents and gravity on a Rivlin-Ericksen liquid with a solutal gradient, noting that Hall currents accelerated convection onset, whereas the magnetic field delayed it. Xu [11] explored the nonlinearity of double-diffusive convective drive in Rivlin-Ericksen fluid within a porous matrix, assuming stress-free boundary restrictions. Sharma et al. [12] inspected the influence of Hall currents on compressible Rivlin-Ericksen liquid with solutal gradients under a constant magnetic field. They concluded that Hall currents hastened thermosolutal instability onset, while compressibility, stable solute gradient, and magnetic power delayed it.

Thermosolutal instability in porous media is critical for understanding heat and mass transmission processes in natural and industrial systems. It plays a key role in geothermal energy extraction, petroleum recovery, carbon sequestration, and groundwater management, where temperature and concentration gradients significantly influence fluid flow and stability. Gupta and Sharma [13] analysed thermosolutal convection in a rotary Rivlin-Ericksen liquid with Hall currents, finding that Hall currents and medium permeability expedited instability onset, whereas rotation and magnetic field postponed it. Wang and Tan [14] investigated the initiation of thermosolutal convective motion based on the Brinkman model with a reacting tenure in a horizontally oriented lightly packed permeable medium applying the normal mode analysis. Aggarwal [15] studied thermosolutal convective movement in a rotary permeable matrix containing Rivlin-Ericksen elastic-viscous dusty fluid, revealing that suspended particles and permeability destabilized the system, while rotation and a stable solute gradient stabilized it. Singh and Gupta [16] investigated how fine suspended dusty particles influenced thermosolutal convective drive in compressible Rivlin-Ericksen liquid. They observed that a stable solutal gradient enhanced system stability, while suspended particles accelerated convection onset. Aggarwal and Verma [17] observed the double-diffusive convective motion in a compressible Rivlin-Ericksen liquid with included particles and Hall currents. They instituted that the solutal gradient and magnetic field stabilized convection, while compressibility, included particles, Hall currents, and permeability were destabilizing factors. Kumar et al. [18] studied Veronis-type thermosolutal instability in Rivlin-Ericksen viscoelastic liquid within a permeable medium subjected to unvarying magnetic field. They identified benchmarks for oscillatory waves, which could be either neutrally stable or unstable depending on groupings of free and rigid boundary conditions. Their analysis also extended to Stern-type configurations.

Viscous dissipation presents a crucial role in thermosolutal convection by renovating mechanical energy into heat, which can significantly affect the temperature distribution within the fluid. This phenomenon can either stabilize or destabilize the arrangement reliant on the relative magnitudes of the heat generation and the solute gradient, influencing the onset and evolution of convection in fluid dynamics. Cheng and Wu [19] explored how viscous dissipation influences the launch of convection in longitudinal vortices within the temperature entrance region of a flat parallel channel. Using numerical methods, they focused on the scenario where one plate is consistently heated and the other is consistently chilled. Barletta and Storesletten [20] performed a linear stability analysis of uniform flow in a horizontal porous channel with a rectangular cross-section, investigating thermal

boundary circumstances at the impermeable channel walls, which involved a consistent entering warmth flux at the bottom, constant warmth at the higher, and adiabatic lateral walls. Barletta and Nield [21] studied the combined effects of double-diffusion and viscous dissipation on convective instability in a fluid-saturated porous matrix with horizontal throughflow. Barletta et al. [22] focused on thermal instability in plane Poiseuille movement, particularly examining the influence of viscous dissipation stimulus. Alves et al. [23] re-examined the Prats problem, analysing thermal instability due to small-amplitude distributions overlaid on basic horizontal throughflow in a porous plane layer. Barletta [24] further discovered the role of viscous dissipation as a cause of thermal convection, highlighting how mechanical energy dissipation into heat can trigger convective instabilities. Norouzi et al. [25] investigated the effects of viscous dissipation on thermo-viscous fingering convection, using the finite element method to model the delicacies of viscous fingering in porous matrix and examine the dissipation's role in affecting instability shapes. Requilé [26] analysed the impact of viscous dissipation on Rayleigh-Bénard-Poiseuille/Couette mixed convective currents using linear stability law, considering both the upright heat gradient from exterior boundaries and thermal stratification caused by volumetric heating from dissipation. Sene et al. [27] provided a detailed analysis of the conditions that lead to dissipation-induced thermal instability in the plane Couette movement of a Newtonian liquid with temperature-dependent viscosity. Yadav et al. [28] reconnoitred the combined influence of viscous dissipation and upright throughflow on the initiation of convective motion in a Jeffrey fluid-drenched rotary porous layer. They utilized an enhanced Darcy model to represent the rheological performance of Jeffrey fluid flow within a permeable medium.

The occurrence of a chemical reaction significantly influences thermosolutal instability by altering the concentration gradients and heat distribution within the fluid. Chemical reactions can either stabilize or destabilize the arrangement, reliant on the nature of the reaction (exothermic or endothermic) and its impact on temperature and solute concentration. This interaction affects the onset and evolution of convection, influencing heat and mass transfer processes in various industrial and natural systems, such as in chemical reactors and geophysical flows. Chamkha [29] explored the impacts of a chemical reaction and magnetic power on heat and mass transmission in a heat-producing or absorbing liquid over a continuously moving upright porous surface. Malashetty and Biradar [30] observed the chemically reacting double-diffusive convective drive within an anisotropic permeable layer. The combined power of chemical reactions, warmth and mass transmission, and viscous dissipation on magnetohydrodynamic (MHD) flow over a upright porous wall were analysed by Ahmed et al. [31]. They used the perturbation method. In low-temperature dimethyl ether oxidation, this instability manifests as a transition from uniform plasma to fil-mentation and back to uniformity before ignition as observed by Zhong et al. [32].

The combined influence of chemical reactions and solute gradient on the thermal instability of Rivlin-Ericksen fluids has not been extensively studied, to the best of our awareness. Therefore, an attempt has been made to examine the stability of thermosolutal convective flow in Rivlin-Ericksen fluids, particularly focusing on the influence of chemical reactions and solute gradients, through a porous medium with the inclusion of viscous dissipation influences. This study is unique in its exploration of both linear and nonlinear stability conditions, offering a more comprehensive understanding of how these factors influence the convective behaviour and thermal stability of Rivlin-Ericksen fluids under different physical conditions. By addressing these factors, this research targets to fill a gap in the current literature and provide valuable insights for real-world applications involving viscoelastic fluids, porous media, and chemical reactions.

2. Mathematical construction

Consider an inestimable horizontal reacting porous medium layer of incompressible Rivlin-Ericksen fluid of width L restricted by the planes at $y = 0$ and $y = L$, as exhibited in Fig. 1.

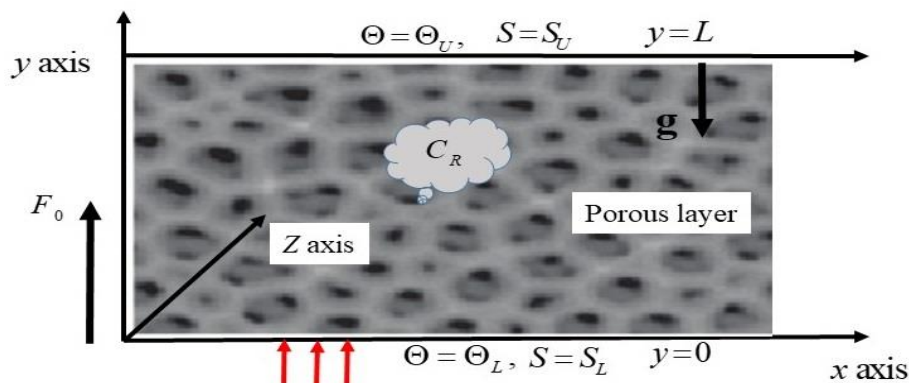


Fig. 1. Physical arrangement of the problem.

This layer is heated from bottom and exposed to a stable solute gradient so that the temperatures and solute concentrations at the lower plane $y = 0$ are Θ_L and S_L , and at the top plane $y = L$ are Θ_U and S_U respectively, with $\Theta_L > \Theta_U$ and $S_L > S_U$. Here, y -axis is considered as vertical such that the gravity force $\mathbf{g} = -g\hat{\mathbf{e}}_y$ permeates the system. It is anticipated that there presents a homogeneous chemical reaction among the Rivlin-Ericksen liquid and the species concentration of rate C_R . Further, the permeable layer is enthused by the uniform upright throughflow of strength F_0 . On using the amended Rivlin-Ericksen-Darcy model and the Boussinesq guesstimate with the influence of viscous dissipation contribution in the energy balance equation, the prevailing equations of the arrangement can be stated as [12, 13, 21, 33-35]:

$$\nabla \cdot \mathbf{U}_D = 0, \quad (1)$$

$$\left(\mu + \dot{\mu} \frac{\partial}{\partial \tau} \right) \frac{\mathbf{U}_D}{M} = -\nabla P + \rho_0 g \left\{ \beta_\Theta (\Theta - \Theta_U) + \beta_S (S - S_U) \right\} \hat{\mathbf{e}}_y, \quad (2)$$

$$\left[\eta_1 \frac{\partial}{\partial \tau} + (\mathbf{U}_D \cdot \nabla) \right] \Theta = \alpha \nabla^2 \Theta + \frac{\mu}{M(\rho_0 c)} (\mathbf{U}_D \cdot \mathbf{U}_D), \quad (3)$$

$$\left[\frac{\partial}{\partial \tau} + \frac{1}{\varepsilon} (\mathbf{U}_D \cdot \nabla) \right] S = D_S \nabla^2 S + C_R (S - S_U), \quad (4)$$

where, \mathbf{U}_D shows the Darcy's velocity of the Rivlin-Ericksen fluid, $\nabla \equiv \hat{\mathbf{e}}_x \frac{\partial}{\partial x} + \hat{\mathbf{e}}_y \frac{\partial}{\partial y} + \hat{\mathbf{e}}_z \frac{\partial}{\partial z}$, $\hat{\mathbf{e}}_x$, $\hat{\mathbf{e}}_y$ and $\hat{\mathbf{e}}_z$ signify unit vectors in x , y and z paths, τ terms the time, μ and $\dot{\mu}$ represent the viscosity and viscoelasticity of the Rivlin-Ericksen liquid, respectively, Θ shows the temperature, S symbolizes the solute concentration, ρ_0 specifies the density of the Rivlin-Ericksen fluid at the reference temperature Θ_U , M indicates the porous medium's permeability, P specifies the pressure, β_Θ and β_S signify the thermal and solute extension coefficients, respectively, α signifies the effectual thermal diffusivity of the permeable medium, ε designates the porosity of the porous medium, D_S signifies the mass diffusivity, η_1 indicates the ratio of heat capacities of the Rivlin-Ericksen fluid and effective porous medium, respectively and $(\rho_0 c)$ shows the heat capacity of Rivlin-Ericksen fluid.

The appropriate boundary positions are:

$$\begin{aligned} V = F_0, \quad \Theta = \Theta_L, \quad S = S_L \quad \text{at} \quad y = 0, \\ V = F_0, \quad \Theta = \Theta_U, \quad S = S_U \quad \text{at} \quad y = L. \end{aligned} \quad (5)$$

For non-dimensional examination, we describe the dimensionless variables as:

$$(\bar{x}, \bar{y}, \bar{z}) = \left(\frac{x}{L}, \frac{y}{L}, \frac{z}{L} \right), \quad \bar{\tau} = \frac{\alpha}{\varepsilon L^2} \tau, \quad \bar{P} = \frac{PM}{\mu \alpha}, \quad \bar{\mathbf{U}}_D = \frac{\mathbf{U}_D L}{\alpha}, \quad \bar{\Theta} = \frac{(\Theta - \Theta_U)}{(\Theta_L - \Theta_U)}, \quad \bar{S} = \frac{(S - S_U)}{(S_L - S_U)}. \quad (6)$$

Then, the non-dimensional practice of Eqs. (1)-(5) are:

$$\bar{\nabla} \cdot \bar{\mathbf{U}}_D = 0, \quad (7)$$

$$\left(1 + \gamma \frac{\partial}{\partial \bar{\tau}} \right) \bar{\mathbf{U}}_D = -\bar{\nabla} \bar{P} + R_{DT} \bar{\Theta} \hat{\mathbf{e}}_y + R_{DS} \bar{S} \hat{\mathbf{e}}_y, \quad (8)$$

$$\eta \frac{\partial \bar{\Theta}}{\partial \bar{\tau}} + (\bar{\mathbf{U}}_D \cdot \bar{\nabla}) \bar{\Theta} = \bar{\nabla}^2 \bar{\Theta} + \frac{G_e}{R_{DT}} (\bar{\mathbf{U}}_D \cdot \bar{\mathbf{U}}_D), \quad (9)$$

$$\frac{\partial \bar{S}}{\partial \bar{\tau}} + (\bar{\mathbf{U}}_D \cdot \bar{\nabla}) \bar{S} = \left(\frac{1}{Le} \bar{\nabla}^2 + K_{CR} \right) \bar{S}, \quad (10)$$

$$\begin{aligned} \bar{V}_D &= Pe, \bar{\Theta} = 1, \bar{S} = 1 \quad \text{at } \bar{y} = 0, \\ \bar{V}_D &= Pe, \bar{\Theta} = 0, \bar{S} = 0 \quad \text{at } \bar{y} = 1. \end{aligned} \tag{11}$$

Here, $\bar{\nabla}^2 \equiv \frac{\partial^2}{\partial \bar{x}^2} + \frac{\partial^2}{\partial \bar{y}^2} + \frac{\partial^2}{\partial \bar{z}^2}$, $R_{DT} = \frac{\rho_0 g \beta_\Theta (\Theta_L - \Theta_U) ML}{\mu \alpha}$ (thermal Darcy–Rayleigh number),
 $R_{DS} = \frac{\rho_0 g \beta_S (S_L - S_U) ML}{\mu \alpha}$ (solutal Darcy–Rayleigh number), $\eta = \frac{\eta_1}{\varepsilon}$ (modified heat capacity ratio),
 $\gamma = \frac{\dot{\mu} \alpha}{\mu \varepsilon L^2}$ (Rivlin-Ericksen parameter), $Le = \frac{\alpha}{\varepsilon D_S}$ (Lewis number), $K_{CR} = \frac{\varepsilon C_R L^2}{\alpha}$ (chemical reaction parameter), $G_e = \frac{g \beta_\Theta L}{c}$ (Gebhart number) and $Pe = \frac{F_0 L}{\alpha}$ (Péclet number).

2.1. Basic state flow

The basic state flow of Rivlin-Ericksen liquid is taken to be free of time, and considered as:

$$\bar{\mathbf{U}}_{Db} = (0, Pe, 0), \bar{\Theta}_b = \bar{\Theta}_b(\bar{y}), \bar{S}_b = \bar{S}_b(\bar{y}). \tag{12}$$

Then, Eqs. (9) - (11) produce for the basic state drive as:

$$\frac{d^2 \bar{\Theta}_b}{d\bar{y}^2} - Pe \frac{d\bar{\Theta}_b}{d\bar{y}} + \frac{G_e}{R_{DT}} Pe^2 = 0, \tag{13}$$

$$\frac{1}{Le} \frac{d^2 \bar{S}_b}{d\bar{y}^2} - Pe \frac{d\bar{S}_b}{d\bar{y}} + K_{CR} \bar{S}_b = 0, \tag{14}$$

$$\begin{aligned} \bar{V}_{Db} &= Pe, \bar{\Theta}_b = 1, \bar{S}_b = 1 \quad \text{at } \bar{y} = 0, \\ \bar{V}_{Db} &= Pe, \bar{\Theta}_b = 0, \bar{S}_b = 0 \quad \text{at } \bar{y} = 1. \end{aligned} \tag{15}$$

On solving Eqs. (13) and (14) with Eq. (15), we have:

$$\bar{\Theta}_b(\bar{y}) = \frac{e^{Pe} - e^{Pe\bar{y}}}{e^{Pe} - 1} - \frac{EcPe(-1 + e^{Pe\bar{y}} + \bar{y} - e^{Pe}\bar{y})}{(e^{Pe} - 1)}, \tag{16}$$

$$\bar{S}_b(\bar{y}) = \frac{-e^{\frac{1}{2}\left(LePe + \sqrt{Le(-4K_{CR} + LePe^2)}\right)\bar{y}} + e^{\frac{1}{2}\left(LePe - \sqrt{Le(-4K_{CR} + LePe^2)}\right)\bar{y}}}{-1 + e^{\sqrt{Le(-4K_{CR} + LePe^2)}}}. \tag{17}$$

Here, $Ec = \frac{G_e}{R_{aD}}$ is the Darcy–Eckert number. The result presented in the Eq. (16) is identical with the outcome achieved by Barletta et al. [36]. In the absence of throughflow ($Pe \rightarrow 0$), Eqs. (16) and (17) provide:

$$\bar{\Theta}_b(\bar{y}) = 1 - \bar{y}, \tag{18}$$

$$\bar{S}_b(\bar{y}) = -\text{csc}\left[\sqrt{K_{CR}Le}\right] \sin\left[\sqrt{K_{CR}Le}(\bar{y} - 1)\right]. \tag{19}$$

The outcome obtainable in the Eqs. (18) and (19) are identical with the consequence achieved by Yadav et al. [33, 34].

In the nonappearance of chemical reaction and viscous dissipation ($K_{CR} \rightarrow 0, Ec \rightarrow 0$), Eqs. (16) and (17) give:

$$\bar{\Theta}_b(\bar{y}) = \frac{e^{Pe} - e^{Pe\bar{y}}}{e^{Pe} - 1}, \quad (20)$$

$$\bar{S}_b(\bar{y}) = \frac{e^{LePe} - e^{LePe\bar{y}}}{e^{LePe} - 1}. \quad (21)$$

The Eqs. (20) and (21) are the same results attained by Nield and Kuznetsov [37] and, Kuznetsov and Nield [38] with scaling of $\bar{S}_b(\bar{y})$.

3. Perturb equations

Here, we implement slight perturbances on the basic state movement as:

$$\bar{P} = \bar{P}_b + \bar{P}', \quad \bar{\mathbf{U}}_D = \bar{\mathbf{U}}_{Db} + \bar{\mathbf{U}}', \quad \bar{\Theta} = \bar{\Theta}_b + \bar{\Theta}', \quad \bar{S} = \bar{S}_b + \bar{S}'. \quad (22)$$

Here, the variables with “dash” superscript are the perturbed dealings on their basic states. On applying Eq. (22) into Eqs. (7)-(11) and eradicating the pressure tenure, we have:

$$\left(1 + \gamma \frac{\partial}{\partial \bar{\tau}}\right) \bar{\nabla}^2 \bar{V}' = R_{DT} \bar{\nabla}_H^2 \bar{\Theta}' + R_{DS} \bar{\nabla}_H^2 \bar{S}', \quad (23)$$

$$\eta \frac{\partial \bar{\Theta}'}{\partial \bar{\tau}} + (\bar{\mathbf{U}}' \cdot \bar{\nabla}) \bar{\Theta}' + \bar{V}' \frac{\partial \bar{\Theta}_b}{\partial \bar{y}} + Pe \frac{\partial \bar{\Theta}'}{\partial \bar{y}} = \bar{\nabla}^2 \bar{\Theta}' + \frac{G_e}{R_{DT}} (\bar{\mathbf{U}}' \cdot \bar{\mathbf{U}}') + 2 \frac{G_e Pe}{R_{DT}} \bar{V}', \quad (24)$$

$$\frac{\partial \bar{S}'}{\partial \bar{\tau}} + (\bar{\mathbf{U}}' \cdot \bar{\nabla}) \bar{S}' + \bar{V}' \frac{\partial \bar{S}_b}{\partial \bar{y}} + Pe \frac{\partial \bar{S}'}{\partial \bar{y}} = \left(\frac{1}{Le} \bar{\nabla}^2 + K_{CR}\right) \bar{S}', \quad (25)$$

$$\bar{V}' = 0, \quad \bar{\Theta}' = 0, \quad \bar{S}' = 0 \quad \text{at } \bar{y} = 0, 1. \quad (26)$$

$$\text{Here } \bar{\nabla}_H^2 \equiv \frac{\partial^2}{\partial \bar{x}^2} + \frac{\partial^2}{\partial \bar{z}^2}.$$

4. Linear stability investigation

In this segment, we discover the onsets for the convective movement applying the linear concept. Now, we take that the amounts of the perturbation are actual slight and can be considered as [39-48]:

$$(\bar{V}', \bar{\Theta}', \bar{S}') = (\tilde{V}, \tilde{\Theta}, \tilde{S})(\bar{y}) e^{ia_x \bar{x} + ia_z \bar{z} + i\sigma \bar{\tau}}, \quad (27)$$

where σ signifies the rate of turbulences and, a_x and a_y are wave numbers in the trend of x and z ways, respectively. On using Eq. (27) into Eqs. (23)-(26) and avoidance the nonlinear tenures with perturbed flexibles, we have:

$$(1 + \gamma i\sigma)(D^2 - \delta^2) \tilde{V} + \delta^2 R_{DT} \tilde{\Theta} + \delta^2 R_{DS} \tilde{S} = 0, \quad (28)$$

$$\eta i\sigma \tilde{\Theta} + \tilde{V} D \bar{\Theta}_b + Pe D \tilde{\Theta} = (D^2 - \delta^2) \tilde{\Theta} + 2 \frac{G_e Pe}{R_{DT}} \tilde{V}, \quad (29)$$

$$-\tilde{V} D \bar{S}_b + \left[\frac{1}{Le}(D^2 - \delta^2) + K_{CR} - Pe D - i\sigma\right] \tilde{S} = 0, \quad (30)$$

$$\tilde{V} = 0, \quad \tilde{\Theta} = 0, \quad \tilde{S} = 0 \quad \text{at } \bar{y} = 0, 1. \quad (31)$$

Here $\frac{d}{d\bar{y}} \equiv D$ and $\delta = \sqrt{a_x^2 + a_y^2}$ is the resulting wave number.

The Galerkin method of weighted residuals technique is applied to get a closed form solution to the arrangement of Eqs. (28)-(31). The test functions are taken as [49-53]:

$$\tilde{V} = A \sin \pi \bar{y}, \quad \tilde{\Theta} = B \sin \pi \bar{y}, \quad \tilde{S} = C \sin \pi \bar{y}. \quad (32)$$

Here, A , B and C are unidentified coefficients. On substituting Eq. (32), into Eqs. (28)-(30) and performing the orthogonal procedures, three linear algebraic equations are obtained with three unidentified A , B and C . For the incidence of non-singular result, we have:

$$\begin{vmatrix} \frac{J_1}{2}(-1-i\gamma\sigma) & \frac{1}{2}\delta^2 R_{DT} & \frac{1}{2}\delta^2 R_{DS} \\ \frac{G_e Pe^3 + 8G_e Pe\pi^2 + 4\pi^2 R_{DT}}{2Pe^2 R_{DT} + 8\pi^2 R_{DT}} & \frac{1}{2}(-J_1 - i\eta\sigma) & 0 \\ J_3 & 0 & -\frac{(J_1 + i\sigma Le - K_{CR} Le)}{2Le} \end{vmatrix} = 0. \quad (33)$$

Here $J_1 = \pi^2 + \delta^2$, $J_2 = \sqrt{Le(-4K_{CR} + LePe^2)}$ and

$$J_3 = \frac{8\pi^2 \left[(e^{J_2} - 1)J_2^2 + 2J_2 LePe \left(1 + e^{J_2} - 2e^{\frac{1}{2}(J_2 + LePe)} \right) + (e^{J_2} - 1)(Le^2 Pe^2 + 16\pi^2) \right]}{(e^{J_2} - 1) \left[J_2^4 + (Le^2 Pe^2 + 16\pi^2)^2 + J_2^2 (-2Le^2 Pe^2 + 32\pi^2) \right]}.$$

On solving Eq. (33) for R_{DT} , we have:

$$R_{DT} = J_4 + i\sigma J_5. \quad (34)$$

Here,

$$J_4 = -\frac{-J_1^2 (Pe^2 + 4\pi^2) + \gamma J_1 \eta \sigma^2 (Pe^2 + 4\pi^2) + \delta^2 G_e Pe (Pe^2 + 8\pi^2)}{4\delta^2 \pi^2} - \frac{J_3 Le (J_1^2 - J_1 K_{CR} Le + Le \eta \sigma^2) (Pe^2 + 4\pi^2) R_{DS}}{2[(J_1 - K_{CR} Le)^2 + Le^2 \sigma^2] \pi^2}$$

and $J_5 = \frac{(Pe^2 + 4\pi^2) \left[J_1 (\gamma J_1 + \eta) \left\{ (J_1 - K_{CR} Le)^2 + Le^2 \sigma^2 \right\} + 2\delta^2 J_3 Le \left\{ J_1 (Le - \eta) + K_{CR} Le \eta \right\} R_{DS} \right]}{4\delta^2 [(J_1 - K_{CR} Le)^2 + Le^2 \sigma^2] \pi^2}.$

4.1. Nonoscillatory convection

In the circumstance of nonoscillatory convection, we have $\sigma = 0$. Then, Eq. (34) offers the nonoscillatory thermal Darcy-Rayleigh number R_{DT} as:

$$R_{DT} = G_e \left(-2Pe - \frac{Pe^3}{4\pi^2} \right) + \frac{J_1 (Pe^2 + 4\pi^2) (J_1^2 - J_1 K_{CR} Le - 2\delta^2 J_3 Le R_{DS})}{4\delta^2 (J_1 - K_{CR} Le) \pi^2}. \quad (35)$$

The threshold of R_{DT} for the arrival of nonoscillatory convection occurs at the critical wave number δ_c , here $\delta_c = \sqrt{a}$ justifies:

$$\begin{aligned} & (-Pe^2 - 4\pi^2)a^4 + 2(K_{CR} Le - \pi^2)(Pe^2 + 4\pi^2)a^3 - K_{CR} Le (Pe^2 + 4\pi^2) (K_{CR} Le - 2\pi^2 + 2J_3 Le R_{DS}) a^2 \\ & + 2(Pe^2 + 4\pi^2) (-K_{CR} Le \pi^4 + \pi^6) a + \pi^4 (-K_{CR} Le + \pi^2)^2 (Pe^2 + 4\pi^2) = 0. \end{aligned} \quad (36)$$

From Eqs. (35) and (36), it is established that the arrival of nonoscillatory convection does not encouragement by the Rivlin-Ericksen parameter γ . Also from Eq. (36), it is noted that δ_c does not differ on the Gebhart number G_e .

In the lack of throughflow ($Pe \rightarrow 0$), Eqs. (35) and (36) offer:

$$R_{DT} = \frac{(\pi^2 + \delta^2)^2}{\delta^2} - \frac{4LeR_{DS}\pi^2(\delta^2 + \pi^2)}{(\delta^2 + \pi^2 - K_{CR}Le)(4\pi^2 - K_{CR}Le)}, \quad (37)$$

$$E_1 a^4 + 2E_1 E_2 a^3 + (E_2 - \pi^2) \{ E_1 (E_2 + \pi^2) - 4Le\pi^2 R_{DS} \} a^2 - 2\pi^4 E_1 E_2 a - E_1 E_2^2 \pi^4 = 0. \quad (38)$$

Here $E_1 = 4\pi^2 - K_{CR}Le$ and $E_2 = \pi^2 - K_{CR}Le$. The results offered in Eqs. (37) and (38) are same as found by Yadav et al. [34].

In the absence of chemical reacting ($K_{CR} = 0$), Eqs. (37) and (38) become:

$$R_{DT} = \frac{(\pi^2 + \delta^2)^2}{\delta^2} - LeR_{DS}, \quad (39)$$

$$\delta_c = \pi. \quad (40)$$

These are the standard outcomes for a thermosolutal fluid convection in a porous layer [39, 54, 55]. For the single component of regular fluid and absence of viscous dissipation ($R_{DS} = G_e = 0$), Eq. (35) develops:

$$R_{DT} = \frac{(\delta^2 + \pi^2)^2 (4\pi^2 + Pe^2)}{4\pi^2 \delta^2}. \quad (41)$$

This is the matching consequence as developed by Nield and Kuznetsov [56] and Yadav [57].

4.2. Oscillatory convection

The oscillatory design of convective wave happens when $\sigma \neq 0$ and $J_5 = 0$. Then, Eq. (34) provides the oscillatory thermal Darcy-Rayleigh number R_{DT} and the rate of the growth of disturbances σ , respectively as:

$$R_{DT} = - \frac{-J_1^2 (Pe^2 + 4\pi^2) + \gamma J_1 \eta \sigma^2 (Pe^2 + 4\pi^2) + \delta^2 G_e Pe (Pe^2 + 8\pi^2)}{4\delta^2 \pi^2} - \frac{J_3 Le (J_1^2 - J_1 K_{CR} Le + Le \eta \sigma^2) (Pe^2 + 4\pi^2) R_{DS}}{2 [(J_1 - K_{CR} Le)^2 + Le^2 \sigma^2] \pi^2}, \quad (42)$$

$$\sigma^2 = - \frac{1}{Le^2} \left[(J_1 - K_{CR} Le)^2 + \frac{2\delta^2 J_3 Le \{ J_1 (Le - \eta) + K_{CR} Le \eta \} R_{DS}}{J_1 (\gamma J_1 + \eta)} \right]. \quad (43)$$

The convective drive launches as a form of oscillatory style only if $\sigma^2 > 0$. Thus, to get an oscillatory arrival, the analytical result for R_{DT} indicated by Eq. (42) is lessened corresponding to the wave number δ numerically for the condition $\sigma^2 > 0$ for diverse evaluations of involved physical factors and results are displaced via tables and figures.

5. Weak nonlinear exploration

In this division, we execute the weakly nonlinear exploration to find the convective heat and mass transportation, which is accommodating to distinguish the physical appliance of convective flow with less extent of mathematical calculation. For minimalism, we restrain our exploration to two dimensional rolls; accordingly all physical measures are free of \bar{z} which sanctions to present a perturbed no dimension stream function $\bar{\psi}'$ as $\bar{U}' = -\partial \bar{\psi}' / \partial \bar{y}$ and $\bar{V}' = \partial \bar{\psi}' / \partial \bar{x}$. Then, the prevailing Eqs. (23)-(26) with the nonlinear standings are:

$$\left(1 + \gamma \frac{\partial}{\partial \bar{\tau}} \right) \bar{\nabla}^2 \left(\frac{\partial \bar{\psi}'}{\partial \bar{x}} \right) - R_{DT} \bar{\nabla}_H^2 \bar{\Theta}' - R_{DS} \bar{\nabla}_H^2 \bar{S}' = 0, \quad (44)$$

$$\eta \frac{\partial \bar{\Theta}'}{\partial \bar{\tau}} + \left(\frac{\partial \bar{\psi}'}{\partial \bar{x}} \frac{\partial \bar{\Theta}'}{\partial \bar{y}} - \frac{\partial \bar{\psi}'}{\partial \bar{y}} \frac{\partial \bar{\Theta}'}{\partial \bar{x}} \right) + \frac{\partial \bar{\psi}'}{\partial \bar{x}} \frac{\partial \bar{\Theta}'_b}{\partial \bar{y}} + Pe \frac{\partial \bar{\Theta}'}{\partial \bar{y}} - \bar{\nabla}^2 \bar{\Theta}' - \frac{G_e}{R_{DT}} \left\{ \left(\frac{\partial \bar{\psi}'}{\partial \bar{x}} \right)^2 + \left(\frac{\partial \bar{\psi}'}{\partial \bar{y}} \right)^2 \right\} - 2 \frac{G_e Pe}{R_{DT}} \frac{\partial \bar{\psi}'}{\partial \bar{x}} = 0, \tag{45}$$

$$\frac{\partial \bar{S}'}{\partial \bar{\tau}} + \left(\frac{\partial \bar{\psi}'}{\partial \bar{x}} \frac{\partial \bar{S}'}{\partial \bar{y}} - \frac{\partial \bar{\psi}'}{\partial \bar{y}} \frac{\partial \bar{S}'}{\partial \bar{x}} \right) + \frac{\partial \bar{\psi}'}{\partial \bar{x}} \frac{\partial \bar{S}'_b}{\partial \bar{y}} + Pe \frac{\partial \bar{S}'}{\partial \bar{y}} = \left(\frac{1}{Le} \bar{\nabla}^2 + K_{CR} \right) \bar{S}', \tag{46}$$

$$\frac{\partial \bar{\psi}'}{\partial \bar{x}} = 0, \quad \bar{\Theta}' = 0, \quad \bar{S}' = 0 \quad \text{at } \bar{y} = 0, 1. \tag{47}$$

Now, let us describe a minimal double Fourier sequence expressions for the variables under consideration fulfilling the boundary conditions (Eq. (47)) as [58-62]:

$$\bar{\psi}' = A_{11}(\bar{\tau}) \sin(\delta \bar{x}) \sin(\pi \bar{y}), \tag{48}$$

$$\bar{\Theta}' = B_{11}(\bar{\tau}) \cos(\delta \bar{x}) \sin(\pi \bar{y}) + B_{02}(\bar{\tau}) \sin(2\pi \bar{y}), \tag{49}$$

$$\bar{S}' = C_{11}(\bar{\tau}) \cos(\delta \bar{x}) \sin(\pi \bar{y}) + C_{02}(\bar{\tau}) \sin(2\pi \bar{y}). \tag{50}$$

Here, the amplitudes $A_{11}(\bar{\tau})$, $B_{11}(\bar{\tau})$, $B_{02}(\bar{\tau})$, $C_{11}(\bar{\tau})$ and $C_{02}(\bar{\tau})$ depend on time and to be determined. On applying Eqs. (48)-(50) into Eqs. (44)-(46), we achieve the following nonlinear autonomous differential equations:

$$\frac{dA_{11}}{d\bar{\tau}} = \frac{-(\delta^2 + \pi^2) A_{11} + \delta (R_{DT} B_{11} + R_{DS} C_{11})}{\gamma (\delta^2 + \pi^2)}, \tag{51}$$

$$\frac{dB_{11}}{d\bar{\tau}} = \frac{\delta A_{11}}{\eta} \left[\frac{G_e (Pe^3 + 8Pe\pi^2) + 4\pi^2 R_{DT}}{R_{DT} (Pe^2 + 4\pi^2)} + \pi B_{02} \right] - \frac{(\delta^2 + \pi^2) B_{11}}{\eta}, \tag{52}$$

$$\frac{dB_{02}}{d\bar{\tau}} = \frac{-\pi (8\pi B_{02} + \delta A_{11} B_{11})}{2\eta}, \tag{53}$$

$$\frac{dC_{11}}{d\bar{\tau}} = \frac{16\delta\pi^2 \left\{ (e^{J_2} - 1) J_2^2 + 2J_2 LePe \left(1 + e^{J_2} - 2e^{\frac{1}{2}(J_2 + LePe)} \right) + (e^{J_2} - 1) (Le^2 Pe^2 + 16\pi^2) \right\} A_{11}}{(e^{J_2} - 1) \left\{ (J_2 - LePe)^2 + 16\pi^2 \right\} \left\{ (J_2 + LePe)^2 + 16\pi^2 \right\}} - \frac{(\delta^2 - K_{CR} Le + \pi^2) C_{11}}{Le} + \delta\pi A_{11} C_{02}, \tag{54}$$

$$\frac{dC_{02}}{d\bar{\tau}} = \left(K_{CR} - \frac{4\pi^2}{Le} \right) C_{02} - \frac{\delta\pi A_{11} C_{11}}{2}. \tag{55}$$

Here, $J_2 = \sqrt{Le(-4K_{CR} + LePe^2)}$. The analytical resolution of above non-linear equations with time needy variables is too difficult. Therefore, it is needy to crack it numerically exhausting the Runge-Kutta-Fehlberg practice (RKF45). For initial condition, we acquired $A_{11} = 1, B_{11} = B_{02} = C_{11} = C_{02} = 0$. The consequences are also validated with ODE45 function in MATLAB.

5.1. Convective heat and mass transmissions

Here, the Nusselt number Nu and the Sherwood number Sh are defined to compute the convective heat and mass spreads in the system, respectively as:

$$Nu(\bar{\tau}) = 1 + \left[\int_0^{2\pi/\delta} \left(\frac{\partial \bar{\Theta}'}{\partial \bar{y}} \right) d\bar{x} / \int_0^{2\pi/\delta} \left(\frac{\partial \bar{\Theta}_b}{\partial \bar{y}} \right) d\bar{x} \right]_{\bar{y}=0}, \tag{56}$$

$$Sh(\bar{\tau}) = 1 + \left[\int_0^{2\pi/\delta} \left(\frac{\partial \bar{S}'}{\partial \bar{y}} \right) d\bar{x} / \int_0^{2\pi/\lambda} \left(\frac{\partial \bar{S}_b}{\partial \bar{y}} \right) d\bar{x} \right]_{\bar{y}=0}. \tag{57}$$

On using Eqs. (16), (17), (49) and (50) into Eqs. (56) and (57), we have:

$$Nu(\bar{\tau}) = 1 - \frac{2(e^{Pe} - 1)\pi R_{DT} B_{02}}{Pe(Ge(1 - e^{Pe} + Pe) + R_{DT})}, \tag{58}$$

$$Sh(\bar{\tau}) = 1 - \frac{4(e^{J_2} - 1)\pi C_{02}}{J_2 + LePe + e^{J_2}(J_2 - LePe)}. \tag{59}$$

Here $J_2 = \sqrt{Le(-4K_{CR} + LePe^2)}$.

Table 1 Contrast of $R_{DT,c}$, δ_c and σ_c for miscellaneous values of Le , R_{DS} and γ at $\eta = 1.5$, $K_{CR} = 0.2$, $Pe = 0.8$ and $G_e = 0.8$.

R_{DS}	Le	$\gamma = 0.00$			$\gamma = 0.05$			$\gamma = 0.10$			$\gamma = 0.15$		
		$R_{DT,c}$	δ_c	σ_c									
-50	3	123.76	3.13	10.21	128.93	2.93	6.57	140.50	2.75	4.51	153.95	2.64	3.03
	4	111.34	3.12	11.67	109.40	3.02	8.38	115.12	2.85	6.46	123.11	2.73	5.24
	5	100.33	3.12	11.78	95.75	3.08	8.77	98.82	2.91	6.91	104.15	2.79	5.75
	6	90.38	3.12	11.31	85.23	3.11	8.56	87.07	2.95	6.82	90.99	2.83	5.73
-30	3	97.56	3.13	6.81	107.86	2.88	3.40	119.83	3.24	0.00	119.83	3.24	0.00
	4	88.11	3.12	8.54	91.90	2.96	5.74	99.99	2.80	4.16	109.32	2.70	3.09
	5	80.30	3.12	8.81	81.30	3.01	6.28	86.65	2.86	4.83	93.27	2.75	3.90
	6	73.52	3.12	8.54	73.43	3.03	6.22	77.33	2.89	4.89	82.41	2.79	4.04
-10	3	65.84	3.17	0.00	65.84	3.17	0.00	65.84	3.17	0.00	65.84	3.17	0.00
	4	64.88	3.12	3.09	71.10	3.20	0.00	71.10	3.20	0.00	71.10	3.20	0.00
	5	60.27	3.12	4.08	66.78	2.94	2.12	73.97	3.22	0.00	73.97	3.22	0.00
	6	56.67	3.12	4.25	61.56	2.96	2.61	67.54	2.84	1.61	73.79	2.75	0.69
0	3	38.83	3.14	0.00	38.83	3.14	0.00	38.83	3.14	0.00	38.83	3.14	0.00
	4	38.83	3.14	0.00	38.83	3.14	0.00	38.83	3.14	0.00	38.83	3.14	0.00
	5	38.83	3.14	0.00	38.83	3.14	0.00	38.83	3.14	0.00	38.83	3.14	0.00
	6	38.83	3.14	0.00	38.83	3.14	0.00	38.83	3.14	0.00	38.83	3.14	0.00
5	3	25.32	3.13	0.00	25.32	3.13	0.00	25.32	3.13	0.00	25.32	3.13	0.00
	4	22.68	3.11	0.00	22.68	3.11	0.00	22.68	3.11	0.00	22.68	3.11	0.00
	5	21.24	3.11	0.00	21.24	3.11	0.00	21.24	3.11	0.00	21.24	3.11	0.00
	6	20.88	3.10	0.00	20.88	3.10	0.00	20.88	3.10	0.00	20.88	3.10	0.00
7	3	19.92	3.12	0.00	19.92	3.12	0.00	19.92	3.12	0.00	19.92	3.12	0.00
	4	16.22	3.10	0.00	16.22	3.10	0.00	16.22	3.10	0.00	16.22	3.10	0.00
	5	14.20	3.09	0.00	14.20	3.09	0.00	14.20	3.09	0.00	14.20	3.09	0.00
	6	13.69	3.08	0.00	13.69	3.08	0.00	13.69	3.08	0.00	13.69	3.08	0.00

6. Results and discussion

In this effort, we have discovered the inspiration of chemical reaction, the through flow and the viscous dissipation effect on the thermosolutal convective flow of Rivlin-Ericksen liquid through permeable medium. Applying the linear stability conception, the conditions for the onset of nonoscillatory and oscillatory convections were developed analytically in tenures of $R_{DT,c}$ whereas, the convective heat and mass transfer were concluded numerically in terms of Nu and Sh using weakly nonlinear stability exploration. The results are offered in Figs. 2-10 and Tables 1-3. The collection of the involved physical parameters are reserved from the available literature [33].

Fig. 2 shows the deviancies of $R_{DT,c}$, δ_c and σ_c as a efficacy of R_{DS} for diverse evaluations of the Lewis number Le . The outcomes are also recorded in Table 1. From Fig. 2 (i), it is observed that with a boost in the assessments of Le , the critical heat Rayleigh-Darcy number $R_{DT,c}$ decreases for the both nonoscillatory and oscillatory approach of convections. This establishes that the Lewis number Le quickens the inductee of convective flows. This is since the effectual thermal diffusivity of the Rivlin-Ericksen fluid rises with growing Le and this increases the drive of Rivlin-Ericksen liquid movement. From Fig. 2 (i), it is also observed that the assessment of the $R_{DT,c}$ losses on enlarging the assessment of the solutal Rayleigh-Darcy number R_{DS} for both nonoscillatory and oscillatory approaches. This shows that R_{DS} increases the instability of the system. The equivalent result of R_{DS} was also established by Roy et al [63]. From Fig. 2 (ii), it is acknowledged that the critical wave number δ_c increases with increasing the Lewis number Le for oscillatory mode of convection while, this consequence was opposite for nonoscillatory approach of convective flow. From Fig. 2 (ii), it is also perceived that the critical wave number δ_c decreases with increasing the solutal Rayleigh-Darcy number R_{DS} for both nonoscillatory and oscillatory approach of convections. It displays that the size of convective cell upsurges with increasing the solutal Rayleigh-Darcy number R_{DS} . From Fig. 2 (iii), it is distinguished that the oscillatory approach of convection is conceivable only if the estimation of R_{DS} is non-positive and also it relies on the Lewis number Le . The range of R_{DS} at which oscillatory wave happened rises with increasing Le .

The impact of the Rivlin-Ericksen parameter γ on the constancy of the system is offered in Fig. 3. From Fig. 3 (i), it is found that the assessment of $R_{DT,c}$ increases with accumulating the Rivlin-Ericksen parameter γ for the oscillatory mode of convection, while it has no impact on nonoscillatory convection. This show that the increasing γ postpones the arrival of convective current by increasing the viscoelasticity possessions of the Rivlin-Ericksen fluid. From Fig. 3(ii), it is detected that the dimension of the convective cell enhances with the Rivlin-Ericksen parameter γ for the oscillatory approach of convection, whereas it has no impression on nonoscillatory convection. The Rivlin-Ericksen parameter γ also decreases the range of R_{DS} at which the oscillatory wave favored, as detected from Fig. 3 (iii).

Fig. 4 shows the disparities of $R_{DT,c}$, δ_c and σ_c as a occupation of R_{DS} for varied evaluations of the modified heat capacity ratio η . The results are also delivered in Table 2. The influence of η suspensions the occurrence of oscillatory type of convection by increasing $R_{DT,c}$ as detected from Fig. 4 (i). This is for the reason that the energy reinstating capability of the arrangement increases with growing η . From Fig. 4 (ii), it is perceived that the modified heat capacity ratio η increases the extent of convective cells by decreasing δ_c . The modified heat capacity ratio η also diminishes the range of R_{DS} on which the oscillatory approach of convection favored, as established from Fig. 4 (iii). Furthermore, from Fig. 4, it is perceived that the modified heat capacity ratio η has no impression on the nonoscillatory approach of convection.

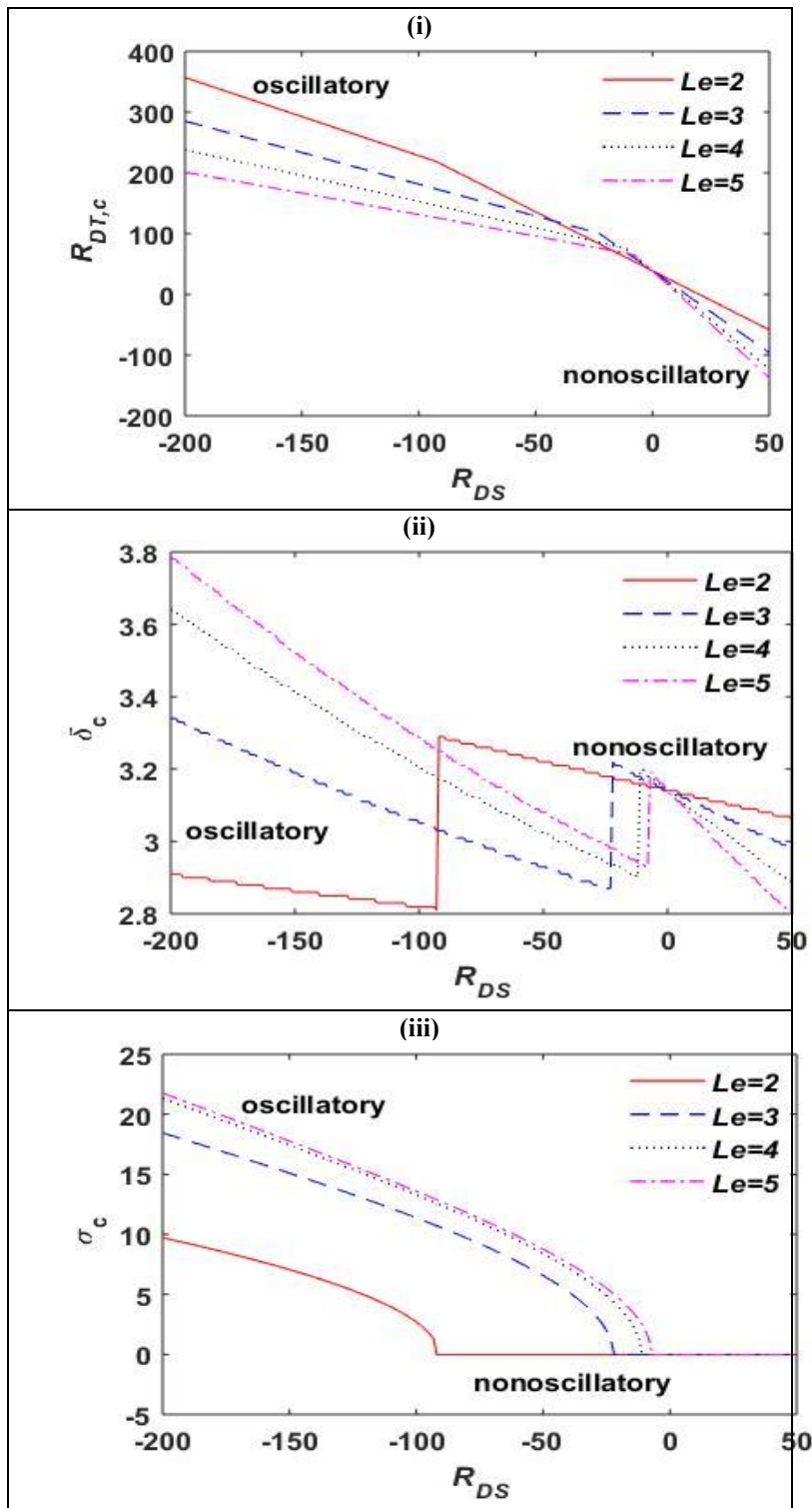


Fig. 2. Discrepancy of $R_{DT,c}$, δ_c and σ_c with R_{DS} for various values of Le at $\gamma = 0.05$, $\eta = 1.5$, $K_{CR} = 0.2$, $Pe = 0.8$ and $G_e = 0.8$.

Table 2 Contrast of $R_{DT,c}$, δ_c and σ_c for miscellaneous values of η , R_{DS} and K_{CR} at $Le = 5, \gamma = 0.05$, $Pe = 0.8$ and $G_e = 0.8$.

R_{DS}	η	$K_{CR} = 0.0$			$K_{CR} = 0.2$			$K_{CR} = 0.4$			$K_{CR} = 0.6$		
		$R_{DT,c}$	δ_c	σ_c									
-50	1	78.12	3.09	11.08	75.30	3.06	10.67	72.01	3.03	10.08	68.11	2.99	9.21
	2	123.93	3.11	7.35	117.49	3.07	7.17	109.81	3.03	6.85	100.53	2.98	6.30
	3	173.24	3.06	4.34	162.83	3.02	4.45	150.36	2.97	4.40	135.20	2.93	4.17
	4	219.61	3.14	0.00	209.33	2.95	1.32	191.91	2.91	1.96	170.68	2.86	2.16
-30	1	69.32	3.02	8.09	67.22	3.00	7.82	64.84	2.97	7.40	62.10	2.95	6.78
	2	100.65	3.03	5.03	96.13	3.00	4.97	90.88	2.97	4.78	84.67	2.93	4.41
	3	134.03	3.00	2.29	126.90	2.97	2.56	118.54	2.93	2.66	108.56	2.89	2.56
	4	147.30	3.14	0.00	144.13	3.37	0.00	137.54	3.58	0.00	126.28	3.75	0.00
-10	1	60.46	2.95	3.45	59.10	2.94	3.41	57.64	2.92	3.26	56.06	2.91	2.96
	2	74.98	3.14	0.00	73.97	3.22	0.00	71.89	2.91	0.53	68.29	3.35	0.00
	3	74.98	3.14	0.00	73.97	3.22	0.00	71.90	3.29	0.00	68.29	3.35	0.00
	4	74.98	3.14	0.00	73.97	3.22	0.00	71.90	3.29	0.00	68.29	3.35	0.00
0	1	38.83	3.14	0.00	38.83	3.14	0.00	38.83	3.14	0.00	38.83	3.14	0.00
	2	38.83	3.14	0.00	38.83	3.14	0.00	38.83	3.14	0.00	38.83	3.14	0.00
	3	38.83	3.14	0.00	38.83	3.14	0.00	38.83	3.14	0.00	38.83	3.14	0.00
	4	38.83	3.14	0.00	38.83	3.14	0.00	38.83	3.14	0.00	38.83	3.14	0.00
5	1	20.75	3.14	0.00	21.24	3.11	0.00	22.23	3.07	0.00	23.97	3.04	0.00
	2	20.75	3.14	0.00	21.24	3.11	0.00	22.23	3.07	0.00	23.97	3.04	0.00
	3	20.75	3.14	0.00	21.24	3.11	0.00	22.23	3.07	0.00	23.97	3.04	0.00
	4	20.75	3.14	0.00	21.24	3.11	0.00	22.23	3.07	0.00	23.97	3.04	0.00
7	1	13.52	3.14	0.00	14.20	3.09	0.00	15.58	3.04	0.00	18.00	3.00	0.00
	2	13.52	3.14	0.00	14.20	3.09	0.00	15.58	3.04	0.00	18.00	3.00	0.00
	3	13.52	3.14	0.00	14.20	3.09	0.00	15.58	3.04	0.00	18.00	3.00	0.00
	4	13.52	3.14	0.00	14.20	3.09	0.00	15.58	3.04	0.00	18.00	3.00	0.00

Fig. 5 offerings the effect of the chemical reaction parameter K_{CR} on the instability of the system. From Fig. 5 (i), it is established that the estimate of $R_{DT,c}$ decreases with K_{CR} for oscillatory mode of convection. It shows that increasing K_{CR} accelerates the onset of oscillatory convective motion, whereas this conclusion is reverse for the nonoscillatory convection. From Fig. 5(ii), it is found that the dimension of convection cell enhances with K_{CR} for both nonoscillatory and oscillatory mode of convections. The chemical reaction parameter K_{CR} has no major impact on the range of R_{DS} on which the oscillatory mode of convection ideal, as detected from Fig. 5 (iii).

The weight of the Péclet number Pe on the instability of the arrangement are presented in Fig. 6. The results are also documented in Table 3. From Fig. 6(i), it is found that the estimation of $R_{DT,c}$ increases with Pe for nonoscillatory approach of convection. It shows that increasing Pe delays the start of nonoscillatory convective motion, whereas this conclusion was contrary for the oscillatory mode of convection. From the Fig. 6 (ii), it is found that extent of the convective cells increases with rising the Péclet number Pe by decreasing δ_c for oscillatory mode of convection, whereas this conclusion was opposed for the nonoscillatory mode of convective drive. The Péclet number Pe also lessens the range of R_{DS} on which the oscillatory approach of convection desired, as recognized from Fig. 6 (iii).

Table 3 Contrast of $R_{DT,c}$, δ_c and σ_c for miscellaneous values of Pe , R_{DS} and G_e at $Le = 5, \gamma = 0.05$, $\eta = 1.5$ and $K_{CR} = 0.2$.

R_{DS}	Pe	$G_e = 0.0$			$G_e = 0.8$			$G_e = 1.6$			$G_e = 2.4$		
		$R_{DT,c}$	δ_c	σ_c									
-50	0	115.32	3.19	11.60	115.32	3.19	11.60	115.32	3.19	11.60	115.32	3.19	11.60
	0.5	105.82	3.13	10.20	105.02	3.13	10.20	104.21	3.13	10.20	103.41	3.13	10.20
	0.6	102.88	3.11	9.73	101.92	3.11	9.73	100.95	3.11	9.73	99.99	3.11	9.73
	0.7	99.92	3.10	9.27	98.80	3.10	9.27	97.67	3.10	9.27	96.54	3.10	9.27
-30	0.0	93.26	3.07	8.42	93.26	3.07	8.42	93.26	3.07	8.42	93.26	3.07	8.42
	0.5	87.66	3.04	7.38	86.86	3.04	7.38	86.05	3.04	7.38	85.25	3.04	7.38
	0.6	85.95	3.03	7.03	84.99	3.03	7.03	84.02	3.03	7.03	83.06	3.03	7.03
	0.7	84.24	3.02	6.66	83.11	3.02	6.66	81.99	3.02	6.66	80.86	3.02	6.66
-10	0.0	71.00	2.96	3.75	71.00	2.96	3.75	71.00	2.96	3.75	71.00	2.96	3.75
	0.5	69.37	2.95	3.02	68.57	2.95	3.02	67.77	2.95	3.02	66.97	2.95	3.02
	0.6	68.91	2.94	2.75	67.95	2.94	2.75	66.98	2.94	2.75	66.02	2.94	2.75
	0.7	68.47	2.94	2.45	67.34	2.94	2.45	66.22	2.94	2.45	65.09	2.94	2.45
0	0.0	39.48	3.14	0.00	39.48	3.14	0.00	39.48	3.14	0.00	39.48	3.14	0.00
	0.5	39.73	3.14	0.00	38.93	3.14	0.00	38.12	3.14	0.00	37.32	3.14	0.00
	0.6	39.84	3.14	0.00	38.87	3.14	0.00	37.91	3.14	0.00	36.95	3.14	0.00
	0.7	39.97	3.14	0.00	38.84	3.14	0.00	37.71	3.14	0.00	36.59	3.14	0.00
5	0.0	12.45	3.08	0.00	12.45	3.08	0.00	12.45	3.08	0.00	12.45	3.08	0.00
	0.5	17.55	3.10	0.00	16.75	3.10	0.00	15.95	3.10	0.00	15.15	3.10	0.00
	0.6	19.18	3.10	0.00	18.22	3.10	0.00	17.26	3.10	0.00	16.29	3.10	0.00
	0.7	20.86	3.10	0.00	19.73	3.10	0.00	18.61	3.10	0.00	17.48	3.10	0.00
7	0.0	1.63	3.06	0.00	1.63	3.06	0.00	1.63	3.06	0.00	1.63	3.06	0.00
	0.5	8.68	3.08	0.00	7.88	3.08	0.00	7.07	3.08	0.00	6.27	3.08	0.00
	0.6	10.92	3.08	0.00	9.95	3.08	0.00	8.99	3.08	0.00	8.03	3.08	0.00
	0.7	13.21	3.09	0.00	12.09	3.09	0.00	10.96	3.09	0.00	9.83	3.09	0.00

Fig. 7 shows the influence the Gebhart number on δ_c and σ_c . From Fig. 7 (i), it is distinguished that an enhance in the estimation of δ_c is to accelerate the convective drive slightly by decreasing the G_e . This ensued because the specific heat capacity of the Rivlin-Ericksen fluid decreases with increasing the Gebhart number G_e . Consequently, the stability of the organism decreases by decreasing the energy restoring capability of system. From Fig. 7(ii) and 7(iii), it is seen that the Gebhart number G_e has no control on the extent of the convection cells and the occurrence of oscillatory mode of convection.

Fig. 8 and Fig. 9 show the impact of R_{DT} , R_{DS} , Le , K_{CR} , Pe , G_e , η and γ on heat and mass transportations in tenures of the Nusselt number Nu and Sherwood number Sh as a utility of the time $\tilde{\tau}$. It is established that the supreme surge of Nu and Sh appearance near to the initial time; it makes spatial activities of progressing frequency. Lastly, the oscillations go to stable form for appropriately huge time. From Fig 8, it is established that the convective heat and mass spreads of arrangement increase with increasing R_{DT} , R_{DS} , Le , K_{CR} , Pe and G_e whereas, from Fig. 9, it is observed that that these spreads of arrangement decrease with increasing η and γ .

Fig. 10 presents the streamlines, isotherms and isohalines with various times. From this figure it is found that the convective cells appear when the convective movement in the arrangement started. From Fig. 10, it is also perceived that with increasing time, the extent of the streamlines and isotherms augmented. Additionally, the isotherms and isohalines are more and more horizontal with growing time.

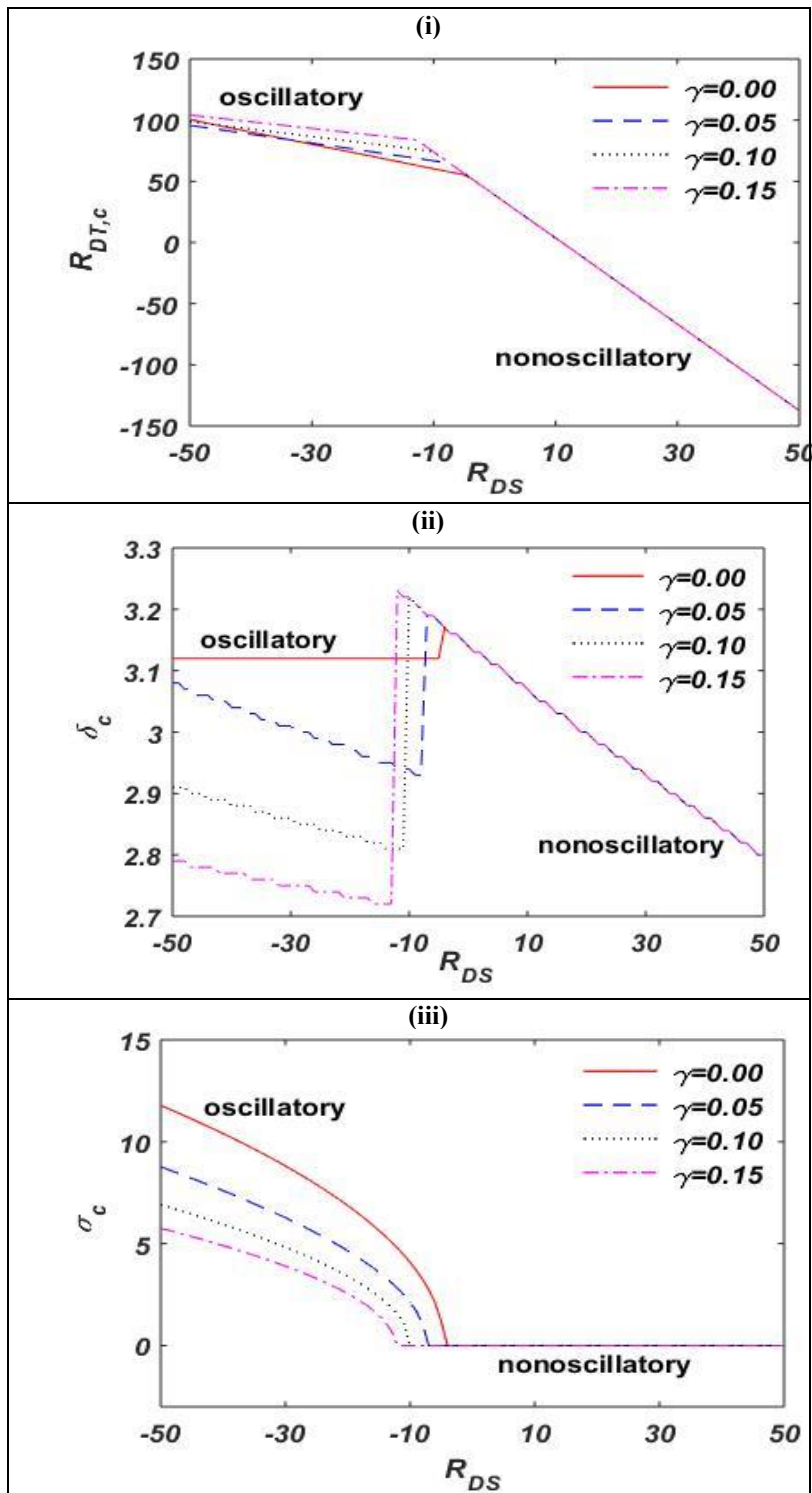


Fig. 3. Disparity of $R_{DT,c}$, δ_c and σ_c with R_{DS} for miscellaneous values of γ at $Le = 5$, $\eta = 1.5$, $K_{CR} = 0.2$, $Pe = 0.8$ and $G_e = 0.8$.

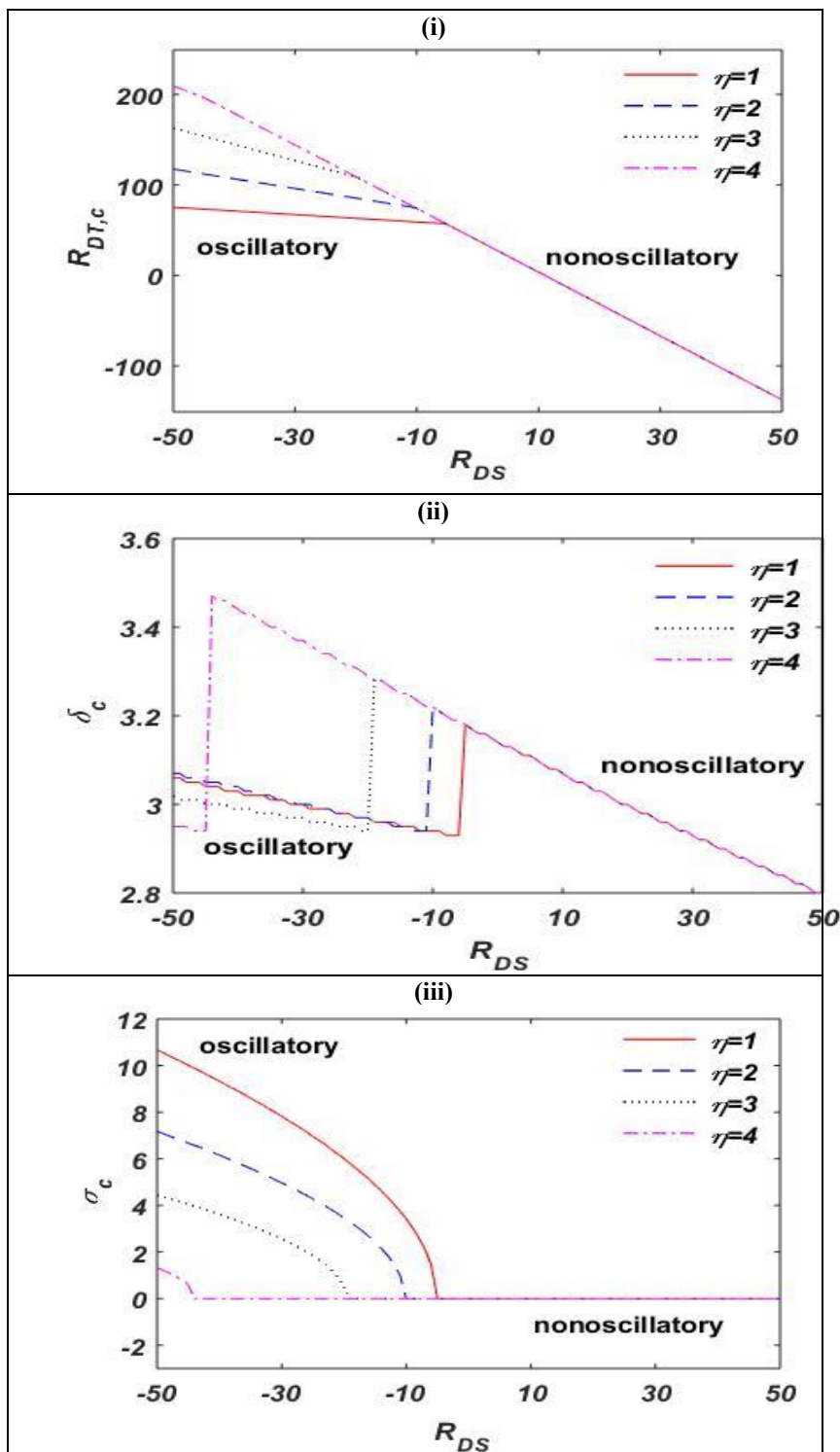


Fig. 4. Disparity of $R_{DT,c}$, δ_c and σ_c with R_{DS} for miscellaneous values of η at $\gamma = 0.05$, $Le = 5$, $K_{CR} = 0.2$, $Pe = 0.8$ and $G_e = 0.8$.

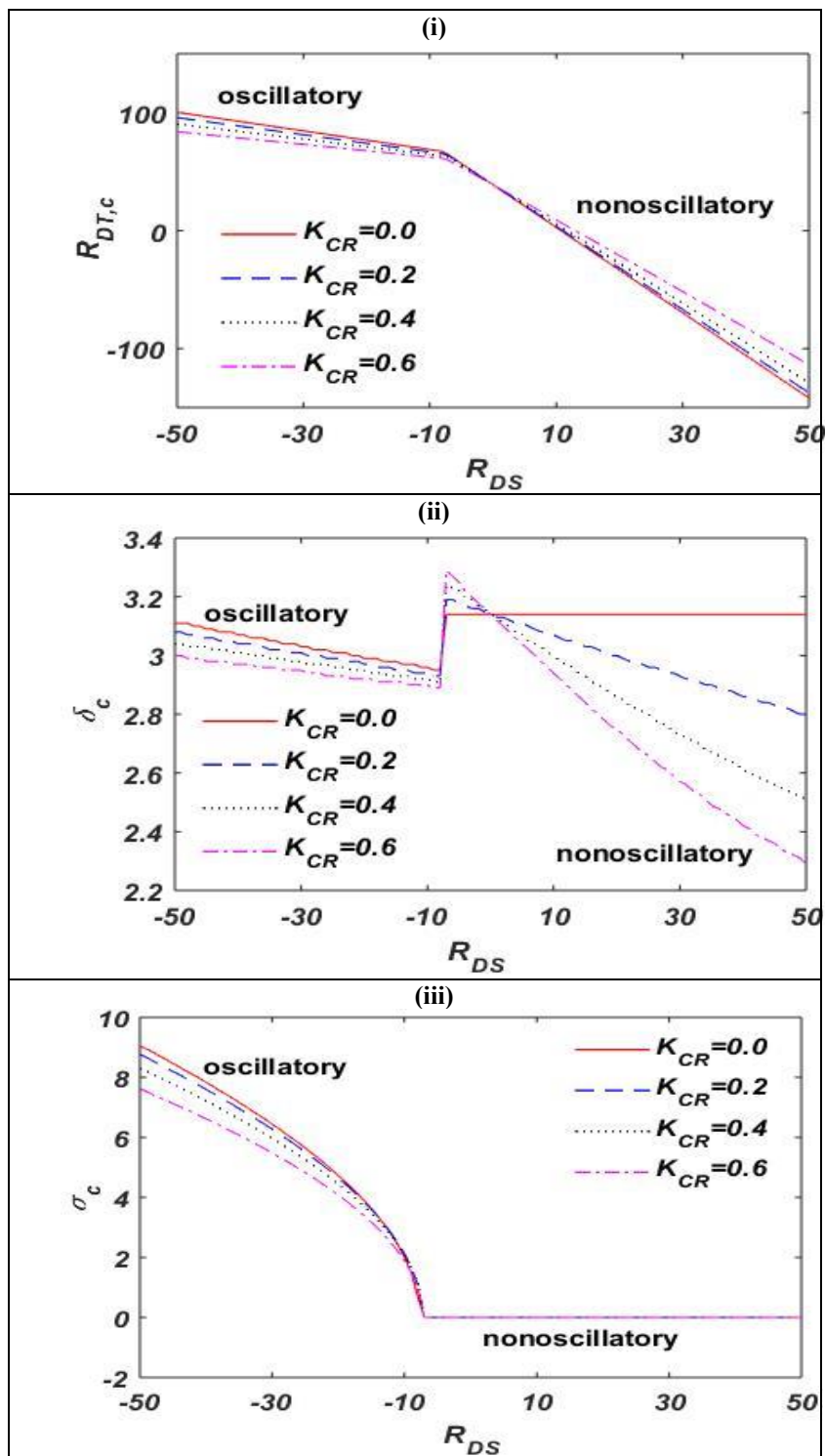


Fig. 5. Disparity of $R_{DT,c}$, δ_c and σ_c with R_{DS} for miscellaneous values of K_{CR} at $\gamma = 0.05$, $Le = 5$, $\eta = 1.5$, $Pe = 0.8$ and $G_e = 0.8$.

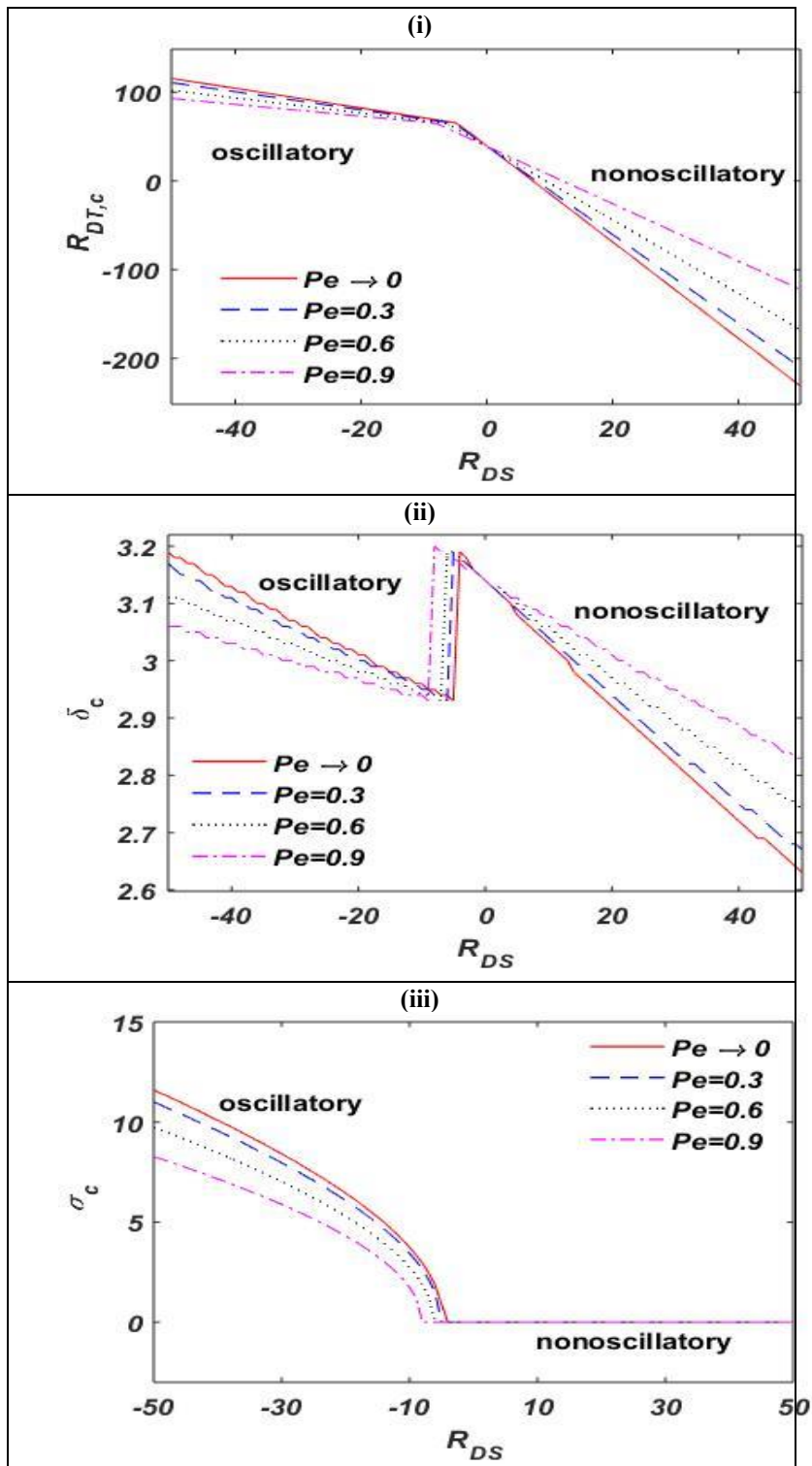


Fig. 6. Disparity of $R_{DT,c}$, δ_c and σ_c with R_{DS} for miscellaneous values of Pe at $\gamma = 0.05$, $Le = 5$, $\eta = 1.5$, $K_{CR} = 0.2$ and $G_e = 0.8$.

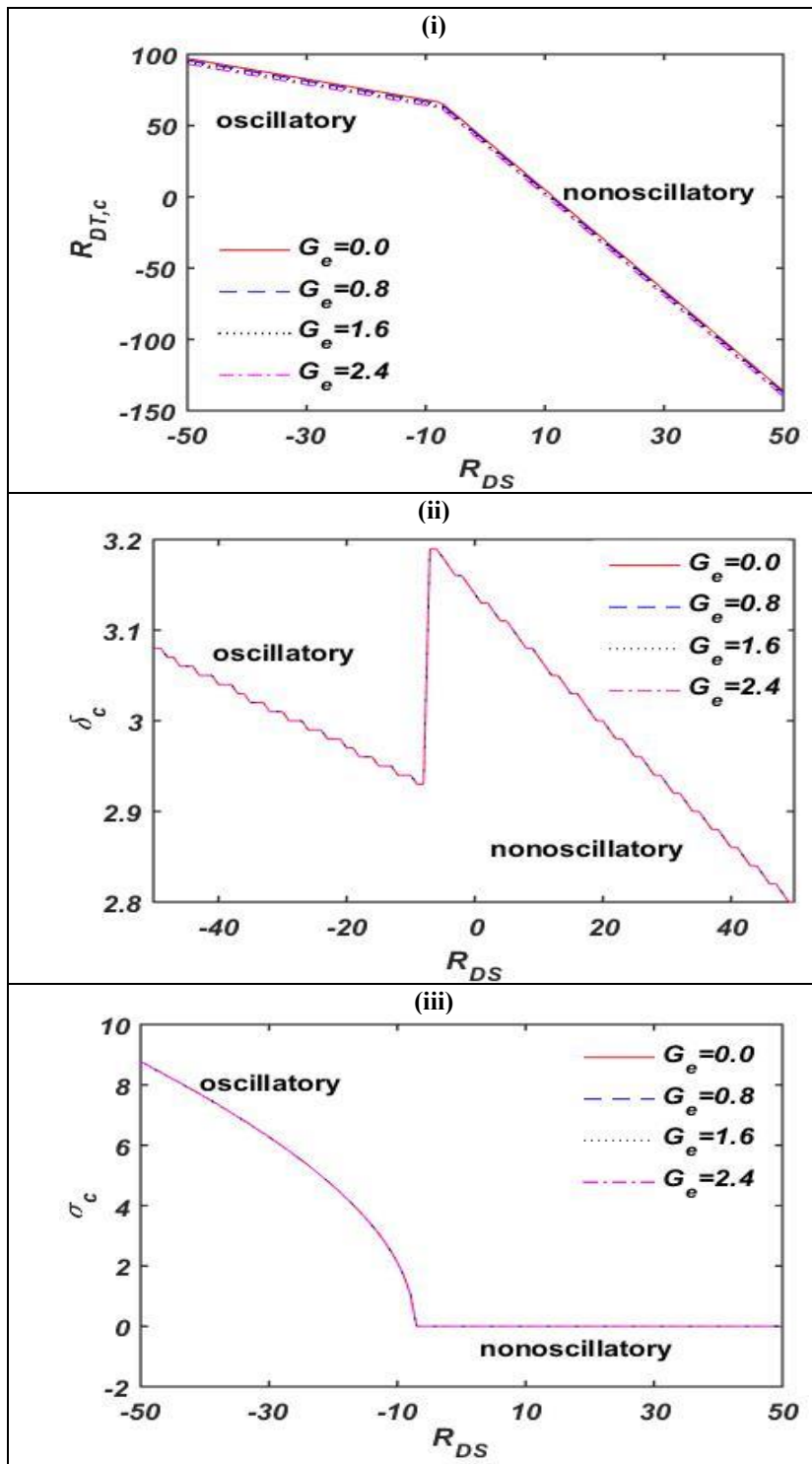


Fig. 7. Disparity of $R_{DT,c}$, δ_c and σ_c with R_{DS} for miscellaneous values of G_e at $\gamma = 0.05$, $Le = 5$, $\eta = 1.5$, $K_{CR} = 0.2$ and $Pe = 0.8$.

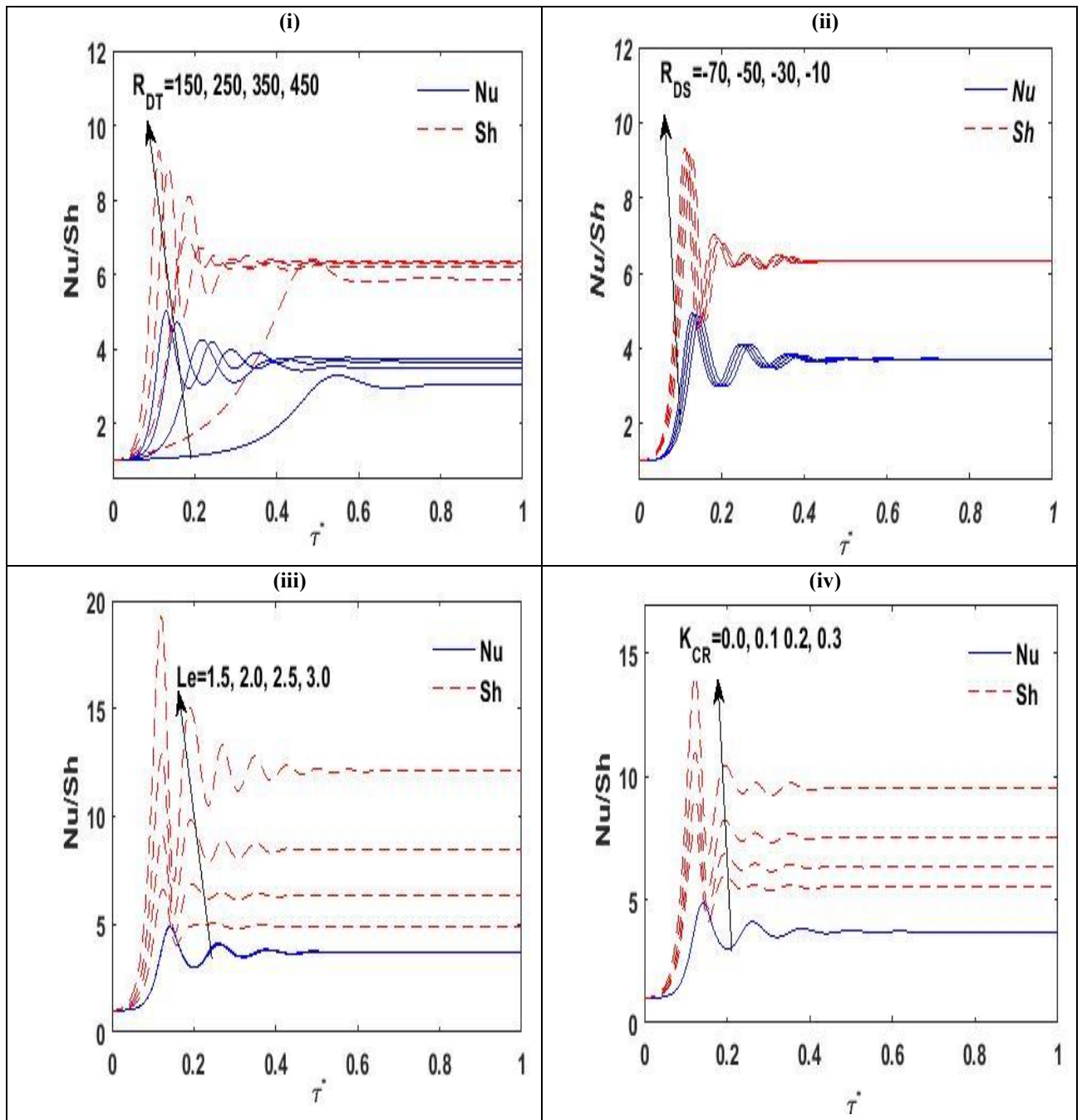


Fig. 8. Variation of the time dependent Nu and Sh with $\bar{\tau}$ for varied values of R_{DT} , R_{DS} , Le , and K_{CR} at $\gamma = 0.05$, $Le = 2$, $\eta = 1.5$, $K_{CR} = 0.1$, $Pe = 0.8$, $G_e = 0.8$, $\delta = 3.1$, $R_{DS} = -50$ and $R_{DT} = 400$.

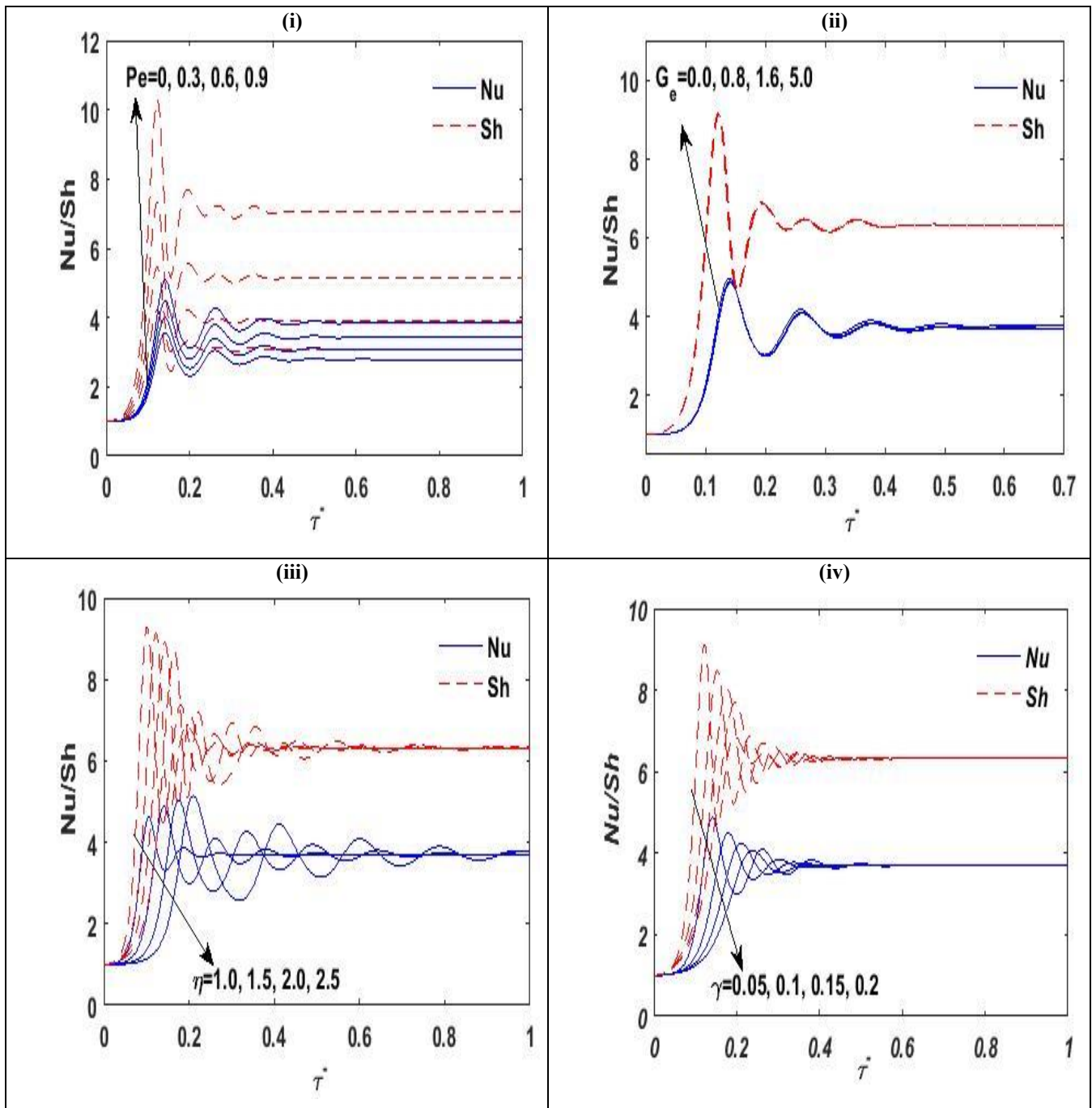


Fig. 9. Variation of the time dependent Nu and Sh with $\bar{\tau}$ for varied values of Pe , G_e , η , and γ at $\gamma = 0.05$, $Le = 2$, $\eta = 1.5$, $K_{CR} = 0.1$, $Pe = 0.8$, $G_e = 0.8$, $\delta = 3.1$, $R_{DS} = -50$ and $R_{DT} = 400$.

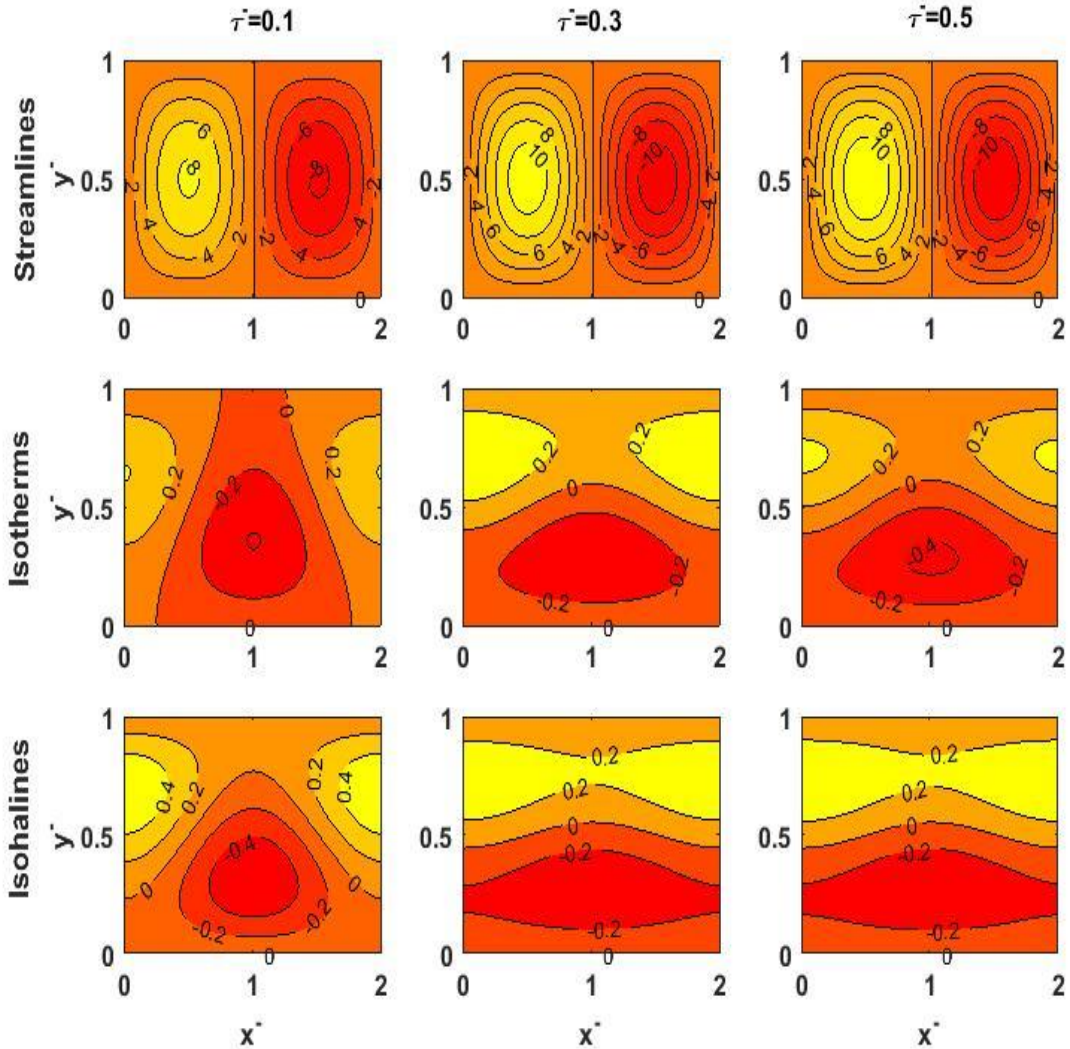


Fig. 10. Streamlines, isotherms and isohalines with miscellaneous time at $\gamma = 0.05$, $Le = 2$, $\eta = 1.5$, $K_{CR} = 0.2$, $Pe = 0.8$, $G_e = 0.8$, $\delta = 3.1$, $R_{DS} = -50$ and $R_{DT} = 400$.

7. Conclusions

In this analysis, the power of the chemical reaction, the through flow and the viscous dissipation on the thermosolutal convective flow of Rivlin-Ericksen fluid through porous medium was analyzed using linear and weak nonlinear constancies theories. The core outcomes of this analysis are itemized as:

- The assortment of the solutal Rayleigh-Darcy number R_{DS} for which oscillatory mode of convective movement occurred reduces with growing the Rivlin-Ericksen parameter γ , the modified heat capacity ratio η and the Péclet number Pe whereas this range increases with increasing the Lewis number Le .
- The chemical reaction parameter K_{CR} and the Gebhart number G_e have no impact on the occurrence of oscillatory mode of convective movement.

- The oscillatory approach of convective movement is feasible only if the assessment of the solutal Rayleigh-Darcy number R_{DS} is negative.
- The Lewis number Le , the solutal Rayleigh-Darcy number R_{DS} and the Gebhart number G_e hurry the commencement of convective wave, while the Rivlin-Ericksen parameter γ and the modified heat capacity ratio η postponement it. Further, the chemical reaction parameter K_{CR} and the Péclet number Pe accelerate the oscillatory convective motion while the nonoscillatory convective motion delay with increasing K_{CR} and Pe .
- The dimension of the convective cell increases with cumulating the Rivlin-Ericksen parameter γ , the chemical reaction parameter K_{CR} and the modified heat capacity ratio η .
- The Rivlin-Ericksen parameter γ , the Gebhart number G_e and the modified heat capacity ratio η have no major influence on the nonoscillatory mode of convection.
- The convective heat and mass spreads of the arrangement upsurge with increasing R_{DT} , R_{DS} , Le , K_{CR} , Pe and G_e whereas, this result was opposite with increasing η and γ .

References

- [1] R. Rivlin, J. Ericksen, Stress deformation relation for isotropic materials, *J. Rational Mech. Anal.*, Vol. 4, pp. 323-329, 1955.
- [2] R. C. Sharma, P. Kumar, Effect of rotation on thermal instability in Rivlin-Ericksen elastico-viscous fluid, *Zeitschrift für Naturforschung A*, Vol. 51, No. 7, pp. 821-824, 1996.
- [3] R. Sharma, P. Kumar, Thermal instability in Rivlin-Ericksen elastico-viscous fluids in hydromagnetics, *Zeitschrift für Naturforschung A*, Vol. 52, No. 4, pp. 369-371, 1997.
- [4] R. Sharma, P. Kumar, Hydromagnetic stability of two Rivlin-Ericksen elastico-viscous superposed conducting fluids, *Zeitschrift für Naturforschung A*, Vol. 52, No. 6-7, pp. 528-532, 1997.
- [5] R. Sharma, S. Kango, Thermal convection in Rivlin-Ericksen elastico-viscous fluid in porous medium in hydromagnetics, *Czechoslovak journal of physics*, Vol. 49, No. 2, pp. 197-203, 1999.
- [6] R. Sharma, K. Thakur, Hall effect on thermal instability of Rivlin-Ericksen fluid in porous medium, *Applied Mechanics and Engineering*, Vol. 5, No. 2, pp. 355-366, 2000.
- [7] U. Gupta, G. Sharma, On Rivlin-Erickson elastico-viscous fluid heated and soluted from below in the presence of compressibility, rotation and Hall currents, *Journal of Applied Mathematics and Computing*, Vol. 25, pp. 51-66, 2007.
- [8] S. Kango, V. Singh, Thermal Instability of Rivlin-Ericksen elastico-viscous rotating fluid in porous medium in hydromagnetics, *Applications and Applied Mathematics: An International Journal (AAM)*, Vol. 7, No. 1, pp. 248-260, 2012.
- [9] R. Sharma, S. Chand, Thermosolutal convection in Rivlin-Ericksen fluid in porous medium in hydromagnetics, *Applied Mechanics and Engineering*, Vol. 3, No. 1, pp. 171-180, 1998.
- [10] V. Sharma, K. Kishor, Hall effect on thermosolutal instability of Rivlin-Ericksen fluid with varying gravity field in porous medium, *Indian journal of pure and Applied Mathematics*, Vol. 32, No. 11, pp. 1643-1658, 2001.
- [11] L. Xu, Energy criterion of nonlinear stability of a flow of the Rivlin-Ericksen fluid in porous medium, *Communications in Nonlinear Science and Numerical Simulation*, Vol. 7, No. 4, pp. 165-173, 2002.
- [12] Y. Sharma, P. Bharti, R. Sharma, Thermosolutal instability of compressible Rivlin-Ericksen fluid with Hall currents, *International Journal of Applied Mechanics and Engineering*, Vol. 10, No. 2, pp. 329-343, 2005.
- [13] U. Gupta, G. Sharma, Thermosolutal instability of a compressible Rivlin-Erickson fluid in the presence of rotation and Hall currents saturating a porous medium, *Applied mathematics and computation*, Vol. 196, No. 1, pp. 158-173, 2008.
- [14] S. Wang, W. Tan, The onset of Darcy-Brinkman thermosolutal convection in a horizontal porous media, *Physics Letters A*, Vol. 373, No. 7, pp. 776-780, 2009/02/16/, 2009.
- [15] A. Aggarwal, Effect of rotation on thermosolutal convection in a Rivlin-Ericksen fluid permeated with suspended particles in porous medium, *Advances in Theoretical and Applied Mechanics*, Vol. 3, No. 4, pp. 177-188, 2010.
- [16] M. Singh, R. K. Gupta, Double-Diffusive Convection in Presence of Compressible Rivlin-Ericksen Fluid with Fine Dust, *Journal of Fluids*, Vol. 2014, No. 1, pp. 714150, 2014.

- [17] A. Aggarwal, A. Verma, Effect of Hall currents on double diffusive convection of compressible Rivlin-Ericksen fluid permeated with suspended particles in porous medium, in *Proceeding of*, AIP Publishing, pp.
- [18] P. Kumar, A. S. Banyal, N. Singh, Magneto-Thermosolutal Convection in Rivlin-Ericksen Viscoelastic Fluid in a Porous Medium, *Research Journal of Science and Technology*, Vol. 9, No. 1, pp. 101-110, 2017.
- [19] K. Cheng, R.-S. Wu, Viscous dissipation effects on convective instability and heat transfer in plane Poiseuille flow heated from below, *Applied Scientific Research*, Vol. 32, pp. 327-346, 1976.
- [20] A. Barletta, L. Storesletten, Viscous dissipation and thermoconvective instabilities in a horizontal porous channel heated from below, *International journal of thermal sciences*, Vol. 49, No. 4, pp. 621-630, 2010.
- [21] A. Barletta, D. Nield, Thermosolutal convective instability and viscous dissipation effect in a fluid-saturated porous medium, *International Journal of Heat and Mass Transfer*, Vol. 54, No. 7-8, pp. 1641-1648, 2011.
- [22] A. Barletta, M. Celli, D. Nield, On the onset of dissipation thermal instability for the Poiseuille flow of a highly viscous fluid in a horizontal channel, *Journal of fluid mechanics*, Vol. 681, pp. 499-514, 2011.
- [23] L. d. B. Alves, A. Barletta, S. Hirata, M. Ouarzazi, Effects of viscous dissipation on the convective instability of viscoelastic mixed convection flows in porous media, *International Journal of Heat and Mass Transfer*, Vol. 70, pp. 586-598, 2014.
- [24] A. Barletta, On the thermal instability induced by viscous dissipation, *International Journal of Thermal Sciences*, Vol. 88, pp. 238-247, 2015/02/01/, 2015.
- [25] M. Norouzi, S. Dorrani, H. Shokri, O. A. Bég, Effects of viscous dissipation on miscible thermo-viscous fingering instability in porous media, *International Journal of Heat and Mass Transfer*, Vol. 129, pp. 212-223, 2019.
- [26] Y. Requilé, S. Hirata, M. Ouarzazi, Viscous dissipation effects on the linear stability of Rayleigh-Bénard-Poiseuille/Couette convection, *International Journal of Heat and Mass Transfer*, Vol. 146, pp. 118834, 2020.
- [27] A. Sene, S. Ben Sadek, S. C. Hirata, M. N. Ouarzazi, Onset of viscous dissipation instability in plane Couette flow with temperature-dependent viscosity, *Energies*, Vol. 16, No. 10, pp. 4172, 2023.
- [28] D. Yadav, M. K. Awasthi, R. Ragoju, K. Bhattacharyya, A. Mahajan, J. Wang, Impact of viscous dissipation, throughflow and rotation on the thermal convective instability of Jeffrey fluid in a porous medium layer, *European Journal of Mechanics - B/Fluids*, Vol. 109, pp. 55-65, 2025/01/01/, 2025.
- [29] A. J. Chamkha, Unsteady MHD convective heat and mass transfer past a semi-infinite vertical permeable moving plate with heat absorption, *International journal of engineering science*, Vol. 42, No. 2, pp. 217-230, 2004.
- [30] M. Malashetty, B. S. Biradar, The onset of double diffusive reaction-convection in an anisotropic porous layer, *Physics of Fluids*, Vol. 23, No. 6, pp. 064102, 2011.
- [31] S. Ahmed, J. Zueco, L. M. López-González, Effects of chemical reaction, heat and mass transfer and viscous dissipation over a MHD flow in a vertical porous wall using perturbation method, *International Journal of Heat and Mass Transfer*, Vol. 104, pp. 409-418, 2017.
- [32] H. Zhong, X. Yang, X. Mao, M. N. Shneider, I. V. Adamovich, Y. Ju, Plasma thermal-chemical instability of low-temperature dimethyl ether oxidation in a nanosecond-pulsed dielectric barrier discharge, *Plasma Sources Science and Technology*, Vol. 31, No. 11, pp. 114003, 2022.
- [33] D. Yadav, M. Al-Siyabi, M. K. Awasthi, S. Al-Nadhairi, A. Al-Rahbi, M. Al-Subhi, R. Ragoju, K. Bhattacharyya, Chemical Reaction and Internal Heating Effects on the Double Diffusive Convection in Porous Membrane Enclosures Soaked with Maxwell Fluid, *Membranes*, Vol. 12, No. 3, pp. 338, 2022.
- [34] D. Yadav, M. K. Awasthi, M. Al-Siyabi, S. Al-Nadhairi, A. Al-Rahbi, M. Al-Subhi, R. Ragoju, K. Bhattacharyya, Double diffusive convective motion in a reactive porous medium layer saturated by a non-Newtonian Kuvshinski fluid, *Physics of Fluids*, Vol. 34, No. 2, pp. 024104, 2022.
- [35] K. Roy, R. Ponalagusamy, P. V. S. N. Murthy, The effects of double-diffusion and viscous dissipation on the oscillatory convection in a viscoelastic fluid saturated porous layer, *Physics of Fluids*, Vol. 32, No. 9, 2020.
- [36] A. Barletta, E. Rossi di Schio, L. Storesletten, Convective roll instabilities of vertical throughflow with viscous dissipation in a horizontal porous layer, *Transport in porous media*, Vol. 81, pp. 461-477, 2010.
- [37] D. A. Nield, A. V. Kuznetsov, The Onset of Double-Diffusive Convection in a Vertical Cylinder With Vertical Throughflow, *Journal of Heat Transfer*, Vol. 135, No. 3, 2013.
- [38] A. V. Kuznetsov, D. A. Nield, The Onset of Double-Diffusive Convection in a Vertical Cylinder Occupied by a Heterogeneous Porous Medium with Vertical Throughflow, *Transport in Porous Media*, Vol. 95, No. 2, pp. 327-336, 2012/11/01, 2012.

- [39] D. A. Nield, A. Bejan, 2006, *Convection in porous media*, Springer,
- [40] D. Yadav, Y.-M. Chu, Z. Li, Examination of the nanofluid convective instability of vertical constant throughflow in a porous medium layer with variable gravity, *Applied Nanoscience*, pp. 1-14, 2021.
- [41] D. Yadav, Influence of anisotropy on the Jeffrey fluid convection in a horizontal rotary porous layer, *Heat Transfer—Asian Research*, 2021.
- [42] D. Yadav, U. S. Mahabaleshwar, A. Wakif, R. Chand, Significance of the inconstant viscosity and internal heat generation on the occurrence of Darcy-Brinkman convective motion in a couple-stress fluid saturated porous medium: An analytical solution, *International Communications in Heat and Mass Transfer*, Vol. 122, pp. 105165, 2021/03/01/, 2021.
- [43] D. Yadav, A. A. Mohamad, M. K. Awasthi, The Horton–Rogers–Lapwood problem in a Jeffrey fluid influenced by a vertical magnetic field, *Proceedings of the Institution of Mechanical Engineers, Part E: Journal of Process Mechanical Engineering*, pp. 09544089211031108, 2021.
- [44] D. Yadav, S. Haider, S. Khan, S. Khan, M. M. Selim, Hybrid nanomaterial and instability analysis of convective flow in permeable media, *Applied Nanoscience*, pp. 1-15, 2021.
- [45] D. Yadav, Influence of anisotropy on the Jeffrey fluid convection in a horizontal rotary porous layer, *Heat Transfer*, Vol. 50, No. 5, pp. 4595-4606, 2021.
- [46] R. Chand, D. Yadav, G. Rana, Electrothermo convection in a horizontal layer of rotating nanofluid, *International Journal of Nanoparticles*, Vol. 8, No. 3-4, pp. 241-261, 2015.
- [47] R. Chand, D. Yadav, G. C. Rana, Thermal instability of couple-stress nanofluid with vertical rotation in a porous medium, *Journal of Porous Media*, Vol. 20, No. 7, pp. 635-648, 2017.
- [48] A. Mahajan, R. Nandal, Anisotropic porous penetrative convection for a local thermal non-equilibrium model with Brinkman effects, *International Journal of Heat and Mass Transfer*, Vol. 115, pp. 235-250, 2017.
- [49] D. Yadav, The influence of pulsating throughflow on the onset of electro-thermo-convection in a horizontal porous medium saturated by a dielectric nanofluid, *Journal of Applied Fluid Mechanics*, Vol. 11, No. 6, pp. 1679-1689, 2018.
- [50] D. Nield, A. Kuznetsov, The effect of vertical throughflow on the onset of convection in a porous medium in a rectangular box, *Transport in Porous Media*, Vol. 90, No. 3, pp. 993-1000, 2011.
- [51] D. A. Nield, A. V. Kuznetsov, The onset of convection in a horizontal nanofluid layer of finite depth, *European Journal of Mechanics - B/Fluids*, Vol. 29, No. 3, pp. 217-223, 2010/05/01/, 2010.
- [52] D. Nield, A. Kuznetsov, The onset of convection in a horizontal nanofluid layer of finite depth: a revised model, *International Journal of Heat and Mass Transfer*, Vol. 77, pp. 915-918, 2014.
- [53] D. Yadav, J. Wang, Convective heat transport in a heat generating porous layer saturated by a non-Newtonian nanofluid, *Heat Transfer Engineering*, Vol. 40, No. 16, pp. 1363-1382, 2019.
- [54] R. Chand, G. Rana, Double diffusive convection in a layer of Maxwell viscoelastic fluid in porous medium in the presence of Soret and Dufour effects, *Journal of Fluids*, Vol. 2014, 2014.
- [55] S. Motsa, On the onset of convection in a porous layer in the presence of Dufour and Soret effects, *SAMSA Journal of Pure and Applied Mathematics*, Vol. 3, pp. 58-65, 2008.
- [56] D. Nield, A. Kuznetsov, The effect of pulsating throughflow on the onset of convection in a horizontal porous layer, *Transport in Porous Media*, Vol. 111, pp. 731-740, 2016.
- [57] D. Yadav, The effect of pulsating throughflow on the onset of magneto convection in a layer of nanofluid confined within a Hele-Shaw cell, *Proceedings of the institution of mechanical engineers, Part E: journal of process mechanical engineering*, Vol. 233, No. 5, pp. 1074-1085, 2019.
- [58] D. Yadav, Impact of chemical reaction on the convective heat transport in nanofluid occupying in porous enclosures: A realistic approach, *International Journal of Mechanical Sciences*, Vol. 157-158, pp. 357-373, 2019/07/01/, 2019.
- [59] J. C. Umavathi, M. A. Sheremet, O. Ojjela, G. J. Reddy, The onset of double-diffusive convection in a nanofluid saturated porous layer: Cross-diffusion effects, *European Journal of Mechanics - B/Fluids*, Vol. 65, pp. 70-87, 2017/09/01/, 2017.
- [60] S. N. Gaikwad, S. Kouser, Double diffusive convection in a couple stress fluid saturated porous layer with internal heat source, *International Journal of Heat and Mass Transfer*, Vol. 78, pp. 1254-1264, 2014/11/01/, 2014.
- [61] S. Gaikwad, M. Malashetty, K. R. Prasad, Linear and non-linear double diffusive convection in a fluid-saturated anisotropic porous layer with cross-diffusion effects, *Transport in porous media*, Vol. 80, No. 3, pp. 537-560, 2009.

-
- [62] J. Umavathi, D. Yadav, M. B. Mohite, Linear and nonlinear stability analyses of double-diffusive convection in a porous medium layer saturated in a Maxwell nanofluid with variable viscosity and conductivity, *Elixir Mech Eng*, Vol. 79, pp. 30407-26, 2015.
- [63] K. Roy, R. Ponalagusamy, P. Murthy, The effects of double-diffusion and viscous dissipation on the oscillatory convection in a viscoelastic fluid saturated porous layer, *Physics of Fluids*, Vol. 32, No. 9, pp. 094108, 2020.